ENERGY SYSTEM MODELING OF A HYDROGEN-BASED STEEL PLANT WITH FLEXIBLE OPERATION

Shadi Badreldeen Mohamed Abdalla

A collaborative Master's thesis project between
Delft University of Technology and **DNV**

Public defense: **August 11th, 2025**
Location: **LB01 Snyderstaal**
Time: **14:00**

Graduation Committee

Role	Name	Affiliation and Position
Chair	Laura Ramirez Elizondo	DC Systems, Energy Conversion & Storage – Associate Professor
Core Member 2	Milos Cvetkovic	Intelligent Electrical Power Grids – Associate Professor
Core Member 3	Dennis van der Born	High Voltage Technology Group – Assistant Professor
Advisor	Manfredo Sartori	DC Systems, Energy Conversion & Storage – PhD Student
External Advisor	Thijs Slot	DNV – Head of Section Energy Markets & Strategy

MSc in Sustainable Energy Technology
Faculty of Electrical Engineering, Mathematics and Computer Science
Delft University of Technology

ACKNOWLEDGEMENTS

Praise be to God, by whose grace good deeds are accomplished, by whose grace good deeds and blessings descend, and by whose success goals and objectives are achieved. First and foremost, I would like to extend my thanks and gratitude to my family and friends for their support throughout this journey. This path was filled with ups and downs that was bypassed with their insights and experience. I would also like to thank my Thesis Supervisor Professor, Laura Ramirez Elizondo for supervising my project and ensuring the research is up to academic standards, my Daily Supervisor, Manfredo Sartori for supporting on the smallest hiccups throughout this journey, my Company Supervisor Thijs Slot, for giving me a chance to build this thesis from scratch and ensuring its relevancy in the industry, and the collegues at DNV for providing input to my thesis. Furthermore, I would also like to thank Professor Neslihan Dogan for reassuring my thesis from a metallurgy perspective.

CONTENTS

List of Figures

List of Tables

NOMENCLATURE

Symbol	Definition	Unit
Indices and sets		
i	Production unit index	–
k	Material index	–
f	Final-product index	–
r	Raw-material index	–
t	Time-step index, $t = 1 \dots T$	–
$\mathcal{V}$	Set of all production units	–
$\mathcal{X}$	Mutually-exclusive units	–
$\mathcal{F}$	Flexible-unit set	–
$\mathcal{I}_k^{\text{in}}$	Units that consume material k	–
$\mathcal{I}_k^{\text{out}}$	Units that produce material k	–
$\mathcal{I}_{\text{unt}}$	Uninterruptible units	–
$\mathcal{K}$	Set of all materials	–
$\mathcal{K}_{\text{imd}}$	Non-storable materials	–
$\mathcal{F}$	Final products	–
Decision / state variables		
$s_i[t]$	Start flag of batch in unit i	–
$e_i[t]$	End flag of batch in unit i	–
$x_i[t]$	On/Off state of unit i	–
$u_i[t]$	Material input to unit i	t
$w_i[t]$	Input reduction offered by flexible unit i	t
$y_i[t]$	Material output from unit i	t
$m_k[t]$	Inventory of material k	t
$l_i[t]$	Electrical energy used by unit i	kWh
$M_i[t]$	In-process material in unit i	t
$L[t]$	Total plant energy demand	kWh
$L_{\text{flex}}[t]$	Flexible-energy offer	kWh
$R_{\text{flex}}[t]$	Flexibility revenue	€
$l_{\text{RE}}[t]$	Renewable generation	kWh
$l_{\text{ch}}[t]$	Battery charging power	kW
$l_{\text{dch}}[t]$	Battery discharging power	kW
$b[t]$	Battery mode (1 charge / 0 discharge)	–
$l_{\text{FC}}[t]$	Electricity from fuel cell	kWh
$m_{\text{H}_2\text{–FC}}[t]$	H_2 fed to fuel cell	t
$m_{\text{O}_2\text{–EAF}}[t]$	O_2 used in EAF	t
$l_{\text{EAF–O2}}[t]$	Power saved in EAF via O_2	kWh
$h[t]$	Heating flag (CBI $\rightarrow$ HBI)	–
$l_{\text{hbi}}[t]$	Electric heat for CBI	kWh
Hydrogen-process symbols		
J	Hydrogen fed to reduction shaft	mol (or kg)

Symbol	Definition	Unit
Q	Stoichiometric H_2 for reduction	mol (or kg)
λ	Excess-hydrogen ratio, $\lambda = J/Q$	–
Parameters		
a_i	Batch duration of unit i	time steps
α_i	Minimum batch size	t
β_i	Maximum batch size	t
c_i	Specific electricity use	kWh t^{-1}
d_i	Stand-by electricity	kWh
ϵ	Max. fractional input reduction	–
η_k	Storage capacity for material k	t
B^{full}	Battery capacity	kWh
B^{init}	Initial battery charge	kWh
$l_{\text{ch}}^{\max}$	Max. charge rate	kW
$l_{\text{dch}}^{\max}$	Max. discharge rate	kW
μ	Battery charge efficiency	–
θ	Battery discharge efficiency	–
HHV_{H_2}	Higher heating value of H_2	kWh t^{-1}
FC^{eff}	Fuel-cell efficiency	–
O	EAF saving per t O_2	kWh t^{-1}
$L_{\max}$	Grid-import limit	kW
t_{cool}	Cooling time HBI $\rightarrow$ CBI	h
T	Scheduling Horizon time	h
ϕ_f	Production target for product f	t
$p[t]$	electricity price	€ kWh^{-1}
p_f	Price of product f	€ t^{-1}
p_r	Price of raw material r	€ t^{-1}
p_{CO_2}	Carbon price	€ tCO_2^{-1}
γ_k	Storage cost of material k	€ t^{-1}
$\Omega, \Omega_i, \Omega_{\text{DRI}}$	Big-M constants	–

SUMMARY

In this paper, a batch-based industrial load model is used to model the energy system of a hydrogen-based steel plant. It is formulated in Gorubi as a profit-maximizing Mixed Integer Linear Programming (MILP) problem. The addition of H2 units to the steel plant introduces new operational aspects in steel production. This requires energy efficiency constraints to optimize material usage, considering warm-up time for specific units, and exploring the impact of a fuel cell system with the plant. The existing industrial load model is modified and new constraints are added to obtain flexible behavior, where units have the choice to consume electricity as part of their normal operation or sell the electricity back to the market. 40 scenarios are generated to optimally manage the energy consumption of the plant. Sensitivity analysis reveals that a fuel cell has a low impact on profit in low price periods, hydrogen storage is essential to overcome losses for the assumed average price , and flexible operation achieves the highest profit when encountered with a peak price. After obtaining the energy consumption of the units, they are modeled as loads in Pandapower assuming the worst-case scenario.Then, a time-series load flow analysis is carried out to validate the rating of the main transformer for the radial network. Finally, the peak active and reactive power of the plant is modeled as a static load in a representative European high voltage grid, where load flow reveals that bus voltages and line loadings depend on the location of the plant in the system.

PREFACE

In Micheal Owen's spirit for stating the obvious, I am the student who wrote this thesis so that I can graduate, because graduating is what students do when their thesis is accepted. Born curious, I spent the past two years studying sustainable energy so I could learn more about it—since learning more is how one becomes knowledgeable. When I'm not working towards graduation, I enjoy relaxing in my free time, precisely because free time is for relaxing. By submitting these pages to the committee, I am officially asking to be evaluated, because evaluation is the step that comes before graduation. Should you approve this work, I look forward to graduating—and once I graduate, I will have, by definition, graduated. Stating the obvious,... I would only like to graduate.

Shadi Abdalla and Mr Chatgbt
Delft, August 2025

1

INTRODUCTION

1.1. INTRODUCTION

The energy transition is a collaborative platform where nations worldwide are working to develop and implement sustainable,affordable and reliable solutions.It gained momentum since the climate change agreement in 2015 in Paris, where 196 countries signed a legally binding agreement to limit the increase in global temperature compared to pre-industrial times [1]. To meet this target, global cooperation focused on reducing the greenhouse emissions that contribute to the increase in temperature, and more importantly, eliminating carbon emissions. Nations are developing road maps to decarbonize main sectors such as residential, transportation, and industry. While notable progress can be seen in the residential and transportation sectors, industry fails to stay on track for 2050 vision. In residential, consumers are opting to purchase electricity from renewable generators instead of fossil fuel generators. Mostly, because of cheap electricity when weather conditions are abundant.In addition, contracting carbon-emitting electricity is accompanied by a tax that is usually absorbed by the consumer. In transportation, technological advances in electric vehicles have made it easier to mass-deploy electric cars worldwide. The International Energy Agency[2] reported that worldwide there are almost 25 million Battery Electric Vehicles in 2022, greater by almost 9 million cars compared to 2021. Industry, in particular hard-to-abate sectors such as iron and steel which is usually faced with risk aversion from investors to address their carbon emissions [3].

Hard-to-abate industrial sectors are Iron and Steel; Chemicals; Heavy-Duty Trucks; Shipping; Aviation and Others[4]. Their difficulty in decarbonization arises from the strict requirements in their operation. The challenges associated with industry electrification include electric supply infrastructure costs and constraints, intermittency in renewable sources that do not align with production hours which could increase the operating prices, and risk aversion from industrial companies [3]. Furthermore, the International Renewable Agency (IRENA) [4] has identified technological pathways to decarbonize sectors, these pathways include the use of reduced demand and improved energy

efficiency; direct use of clean electricity; direct use of renewable heat and biomass; indirect use of clean electricity via synthetic fuels; and carbon-dioxide capture, and removal. These pathways are mapped for each sector and classified based on relevance and readiness. Accordingly, utilizing demand-response and clean electricity can potentially map a clear decarbonization pathway for the highest emitting sector, Iron and Steel [4].

Iron and steel are global commodities that are employed in almost every sector. Their demand is expected to increase with increasing quality of life. Accounting for 7% of the global emissions with 2.6 Gt CO_2 emissions[5], the current trajectory of the industry in 2050 is 1.1 tCO_2/steel when it should be 0.6 tCO_2/steel [6].One of the most promising technological pathways to decarbonize iron and steel is to reduce Iron (II) Oxide using hydrogen [7], known as a Hydrogen based Direct Reduction (HD-R). To realize this route, it is essential to model the energy and power system of the HD-R steel plant. Furthermore, operational practices such as flexibility and demand response are introduced to consider electricity prices, which raises the following research questions:

1. What is a suitable model for an industrial steel plant?
2. How can the energy consumption of a hydrogen-based steel plant be optimally managed?
3. How does the Hydrogen-based steel plant affect a High-Voltage transmission grid ?

The rest of the paper is organized as follows. Chapter 2 reviews recent literature in flexible operation of steel plants. Chapter 3 background information for the reader regarding traditional steel-making. Chapter 4 highlights the implemented methodology for the energy and power system modeling. Chapter 5 draws on the result discussion and Chapter 6 concludes the findings of the research.

2

Literature Review

In this paper, flexibility is defined as the ability of an industrial plant to reduce its energy consumption to sell it in the electricity market. The response to demand is the ability of the plant to respond to electricity prices by adjusting its energy consumption schedule. Therefore, it is important to understand how to model the energy system of a steel plant and how flexibilty and demand response are deployed in steel plants. In [8], a basic and flexible Resource Task Network (RTN) was formulated as an MILP was used to evaluate the flexible operation of a Ladle Furance (LF) in a Blast Oxygen Furnace (BOF) steel production route. Flexibility demonstrated production schedules can be met while saving 12000 yuan compared to basic operations. Researchers in [9] developed an MILP that couples energy scheduling and production process to explore the dispatching potential of a steel plant. Flexibility was demonstrated by applying load reduction, interruption and starting times for processes such as the electric arc furnace, air separation system and the steel rolling line. A resource task network was deployed to efficiently schedule the operation of the EAFs as a form of demand response [10]. The authors in [11] formulated an optimization model that identifies sources of flexibility based on renewable generation, On-site generation, steel process and electricity price. They were able to quantify the black starting block and determine the appropriate demand response windows for a 90 MW steel plant in UK. Gholian et al [12], developed a batch-based smart industrial load model that responds to electricity prices and applied to a steel plant based in Iran. In terms of employing hydrogen based steel production, authors in [13] developed an hourly linear cost-minimizing optimization model is implemented in a hydrogen-based steel production plant to determine cost-optimal operation. Results demonstrated that the steel production costs reduced by 17% and 23% when the plant operates in a price-following manner compared to continuous operation. Furthermore, operational costs depend on the electricity mix in the grid. In [14],an open-source mass and energy flow model to investigate the viability of hydrogen in steel production. Combining a hydrogen production plant with a direct reduction shaft and an electric arc furnace, they found that energy consumption in a Hydrogen reduction process is 3.72 MWh/tlS compared to 3.48 MWh/tls from a blast furnace route. More importantly,

the sensitivity analysis indicated that the efficiency of the electrolyzer has a significant impact on the energy consumption profile.Vogl et Al [15]. proposed a hydrogen based steel production plant that is suitable with Alkaline and PEM electrolyzers.The element of flexibility was demonstrated by varying the hydrogen supply to the reduction shaft and varying the scarp and Direct Reduced Iron (DRI) ratio in the EAF. Authors in [16], adopted a minute Resource Task Network formulation to model a cost-effective schedule for a Hydrogen based steel plant. This was used to depict the operation based on a DR Shaft, EAF, transportation, Hydrogen production and storage. Powered by a mixed resource grid, flexibility is investigated in the batch starting time for an electric arc furnace and the scalability of the Proton Exchange Membrane (PEM). Optimal schedule was determined by employing an MILP model that minimizes cost or production time. The previous literature highlights operational characteristics for both hydrogen-based and coke or natural gas powered steel plants.However, they either suffer from at least one of the following limitations. While The papers in [8]–[12] depict operational characteristics by up to final production units, they assume a coke-based steel plant in their case study that is not fully dependent clean energy supply. In the other hand, the operation for Hydrogen-Based steel plants is depicted only until the EAF [13]–[16] without considering units that further process steel into final products.In addition, only [16], is focused on capturing the flexibility of the operation, while the rest of the papers are focused on developing process plants for Hydrogen-based steel production plants.In general, flexible operation can be presented in various forms, it can be in the form managing the production schedule in response to electricity prices [9], [13], [16], or to incentive black start capability in downed grids [11]. It can also be a process ability to reduce its consumption responding to high prices [12]. In this paper, flexibility is defined as a process unit's ability to have two operation modes in a production horizon. Normal operation that is based on the traits of any given unit, and flexible operation that carries the same traits a normal operation, but reduces material consumption as an incentive of selling back electricity to the grid. A summary of the main differences between the previous paper and this work can be seen in Table 2.1

Table 2.1: Comparison of Literature Based on Flexibility and Decarbonization Attributes

Sources	Demand Response	Renewable Generation	Flexibility	Optimal Scheduling	All Process Units	Hydrogen-Based Steel	Battery	Fuel Cell
[8]	✓	✓	✓	✓	✗	✗	✗	✗
[9]	✓	✗	✓	✓	✓	✗	✗	✗
[10]	✓	✗	✗	✓	✗	✗	✗	✗
[11]	✓	✓	✓	✓	✓	✗	✗	✗
[12]	✓	✓	✗	✓	✓	✗	✓	✗
[13]	✓	✓	✗	✓	✗	✓	✗	✗
[14]	✗	✓	✗	✓	✗	✓	✗	✗
[15]	✗	✓	✗	✗	✗	✓	✗	✗
[16]	✓	✓	✓	✓	✗	✓	✗	✗
This Work	✓	✓	✓	✓	✓	✓	✓	✓

Therefore,the research objectives of the paper are listed below:

- Formulating an optimization model that considers the operational constraints associated with each process block, and developing the new constraints associated with integrating the hydrogen plant into the process.

- Analyze the interactions of clean energy supply, hydrogen production as energy storage or input to the steel making process, demand from the steel-making process block and the consumption from the EV actors based on steel logistics.

- Determining the operational flexibilities for the new process that can offer profit in the electricity market

2.1. METHODOLOGY TO ADDRESS RESEARCH QUESTIONS

2.1.1. WHAT IS A SUITABLE ENERGY MODEL FOR AN INDUSTRIAL STEEL PLANT?

The first step is to distinguish between the traits of an industrial load from a residential load [12]. In residential loads, the design factors include peak load shaving, time-shift for the loads, pricing tariffs, renewable generation, energy storage, interruptible and uninterruptible loads. The same traits are found in an industrial load, with the addition of sequential operation, load dependency, size of the batch cycle, number of batch cycle for a process unit, material flow into the process unit, material balance between units, material storage, final product produced, and by-products. By adopting the industrial load framework in [12], a steel plant can be modeled as a smart industrial load. This question is first validated by investigated the scheduled energy consumption of the plant, and ensuring that each unit behaves according to the definition of an industrial load and their is a sequential operation in the steel plant.

2.1.2. HOW TO OPTIMALLY MANAGE THE ENERGY CONSUMPTION OF A HYDROGEN-BASED STEEL PLANT UNDER VARIOUS PRICE SCENARIOS?

Integrating a H_2 plant to a steel process introduced new operational constraints and new ways to explore energy management. The H_2 plant modeled in this paper is from the works of [15]. Accordingly, a fuel cell is adopted to convert stored Hydrogen to electricity.Which requires mathematical constraints such as production rate, efficiency, and capacity. The parameters will be selected from existing manufactured fuel cells. The H_2 plant will adopt the same framework in [12], and specified according to energy efficiency techniques adopted from literature [15], [17]. Furthermore, O_2 supply to the Arc Furnace to reduce the energy consumption is modeled according to the works of [17] . After the Hydrogen-Based steel model is modeled, pricing scenarios are addressed by considering three profiles. They are profiles that each include low, average and peak prices, which are used to answer how a H_2 steel plant owner can optimally manage their energy consumption.

2.1.3. HOW DOES THE HYDROGEN-BASED STEEL PLANT AFFECT A HIGH-VOLTAGE TRANSMISSION GRID?

The profit maximization- produces an energy consumption schedule based on electricity prices. Furthermore, it produces the energy production of the battery and fuel cell. These values are converted to power and modeled in pandapower. Its important to un-

derstand the electrical elements of each of the units. Therefore, a review on the electrical model is conducted by referring to literature and manufacturer datasheet of the process units. A network topology is proposed for the steel plant and static power flow analysis based on the rated power of each unit is carried out. This is carried out to ensure that in the worst case scenario, the main transformer is not overloaded and the bus voltages are operating within acceptable limits. After this is verified, the active and reactive peak power is modeled as a load in a typical European high voltage grid, to understand the impact of the plant on line loadings and bus voltage magnitude.

3

BACKGROUND

3.1. STEEL PRODUCTION ROUTES

Steel is a crucial material that is traded globally with a practical use in every sector. The consumption of steel can be found in car manufacturing, construction, machinery, appliances, infrastructure, and almost every aspect of our lives. The latest report from the World Steel Association reports that in 2022,to produce one tonne of crude steel cast, 20.99 GJ of energy was consumed, which emitted 1.99 tonnes of CO_2 [18]. Its production is a high capital energy intensive process that is failing to avoid carbon emissions. This is mainly because of risk aversion from steel investors, since the overall process of producing steel has more or less remained the same since its discovery.

Steel is an iron-carbon compound that has less than 2.06 % of carbon content [19]. The primary constituent in producing steel is iron, which naturally exists as iron ore (Fe_2O_3).Nowadays, steel is mainly produced from iron ore through reduction or smelting in a Blast Furnace(BF-BOF). Another common way of producing steel is through the Electric Furnace (DR-EAF), which reuses scrap steel or inputs DRI and produces liquid steel. The EAF method is usually adopted by smaller steel plants that produce less quantities of steel compared to BF.This route uses a DR Shaft and natural gas a reducing agent which makes it less emission intensive compared to the BF-BOF route. The DR Shaft is also applicable in Hydrogen based steel, where Hydrogen is used as a reducing agent to produce DRI, this route is known as the Hydrogen Direct Reduced (HD-R DR) route [20]. Figure 3.1 presents a brief overview of steel production routes and known materials.

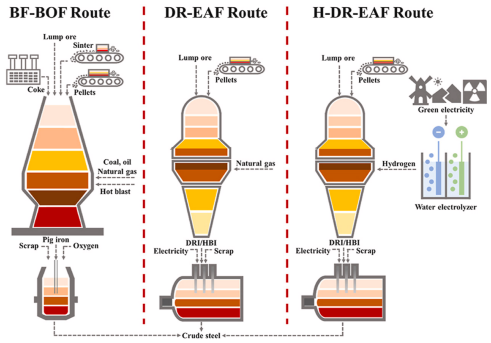

Figure 3.1: Production routes of steel [20]

3.1.1. BF-BOF ROUTE

In the BF route,the first step is to extract iron from iron ore to produce pig iron. As shown in Figure 3.2, this takes place by inserting iron ore pellets, coke and limestone from the top of the blast furnace [19]. The coke acts as a reducing agent that reacts with the oxygen in the ore to produce carbon monoxide and pig iron. The pig iron settles at the bottom of the blast furnace with the impure constituents forming on top of the pig iron, because it has a lower density. The impurities are removed by the limestone and leave the furnace in the form of liquid slag.

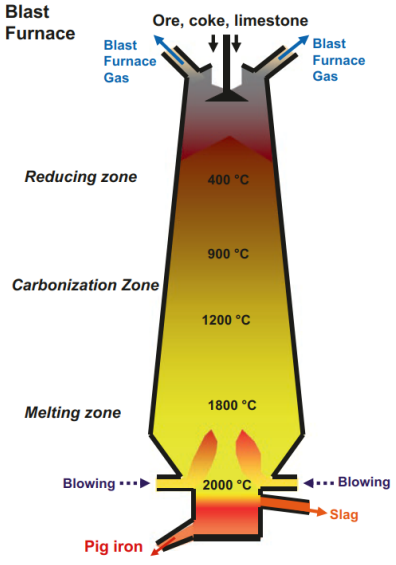

Figure 3.2: Simplified Cross Section of a Blast Furnace with three main zones: reduction, coking, and melting zone [19]

The pig iron steel contains carbon content that is higher than 2%, which requires further processing [19]. This is carried out in the blast converter, where oxygen is blown into the pig iron (liquid) to oxidize the carbon. The output is now raw liquid steel, and once again limestone is added to remove impurities.

3.1.2. DR-EAF ROUTE

Almost 28% of steel production of took place in 2022 via the Electric Arc Furnace route [18]. The EAF melts steel melting raw material such as steel scrap, Direct Reduced Iron(DRI) or both [15], [21].Melting takes place by producing an arc at High current and low voltages [22]. There are various types of furnaces such the arc furnace, induction furnace, resistance furnaces, electron beam furnace, or plasma furnace [23]. Nowadays, more than 90% of steel mills utilize the arc furnace to produce steel batches up to 200 t [19] . *Fig. 3.3* shows a closed cross section of a three-phase electric arc furnace. Steel scrap carried in baskets is loaded (charging) into the furnace from the top, the top lid is then closed. Graphite-electrodes begin to move down and generate an arc between the steel scrap and the electrode, which is used to melt the scrap at 1800°C. The length of the arc depends on the input voltage which requires tap-changing [22]. The graphite- electrode is either carrying an AC or DC current, which takes 30 to 70 minutes to melt the steel scrap completely. The liquid steel is then discharged from the enclosure into a ladle where the next stage of processing begins.

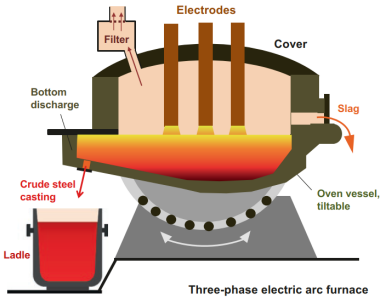

Figure 3.3: Simplified Cross Section of a three-phase electric arc furnace [19]

3.1.3. DR SHAFT

A steel manufacturer may opt to purchase DRI or produce it in-house when they are producing steel via the EAF route. To produce DRI, naturally mined iron-ore is supplied to the DR Shaft along with a reducing agent to produce DRI. The reducing agent is usually natural gas, but cleaner routes are identified through Hydrogen [21]. Furthermore, the iron-ore feed in this process should be classified as high-grade. Figure 3.4 shows a MIDREX DR Shaft process design.

Figure 3.4: MIDREX DR Shaft [24]

3.1.4. HD-R DR ROUTE

Steel produced with hydrogen is identified as one of the most promising routes in decarbonizing the steel industry [14], [15]. In the production of DRI, hydrogen replaces natural gas as a reducing agent and produces water as a by-product instead of CO_2 compared to the DR-EAF route. The carbon emission intensity of this route depends in the electricity supply in the electrolysis process. This route is yet to be seen on a commercial level.However, the Hybrit project in Sweden is currently operating in a pilot stage and is expected to produce green steel commercially in 2026 [25].

3.2. POST-TREATMENT OF STEEL

3.2.1. LADLE FURNACE

Whether it is liquid raw steel coming from the blast furnace or the electric furnace, the ladle furnace is required to post-treat the steel. After liquid steel is produced, its poured into a ladle as shown at the bottom left of Figure 3.3. The post-treatment of this process begins in a ladle stand where the temperature of the liquid steel is maintained and carbon content is set [19]. A more detailed diagram of the ladle furnace is shown in Figure **??**, the three bars are electrodes that produce the arc that is used to maintain the temperature of the melt.

Figure 3.5: Cutaway section of a Ladle Furnace[19]

3.2.2. PRIMARY CASTING

Primary casting or "primary shaping" is a process that shapes the liquid steel by crystallizing the liquid metal to its solid state. There are mainly two ways of casting metals, which are ingot or continuous casting. Currently, more than 90% of steel products are made through continuous casting, and one of the most common shape that is produced is steel slab [19]. Figure 3.6 shows a continuous steel slab caster that operates in batches [26]. Its liquid steel capacity is bounded by the casting limit which sets the processing requirements for molten liquid.

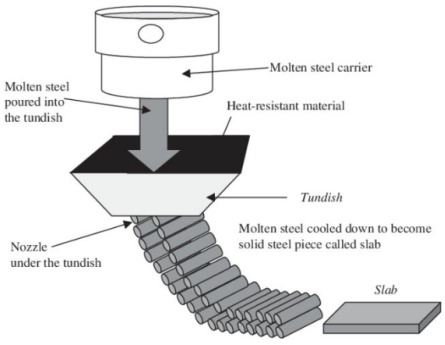

Figure 3.6: Continuous Steel Slab Caster[26]

3.2.3. FORMING

In general, forming is practically deforming, which takes advantage of metals and alloys ability to temporarily deform elastically due to external forces[19]. Its to intentionally tailor a geometric shape from an existing form to a new one. Various methods of forming exist, a few common ones are forging, flow pressing, extrusion, rolling and deep drawing. Particular focus is given to rolling, which produces steel that serves industries such as the maritime, automotive, railway, water infrastructure, and many more applications. Rolling is a pressure forming process that has two or more rolls that rotate in opposite directions. The rotating smooth rolls accepts a steel to narrow its cross-section. The basis of forming through rolling can be seen in Figure 3.7.

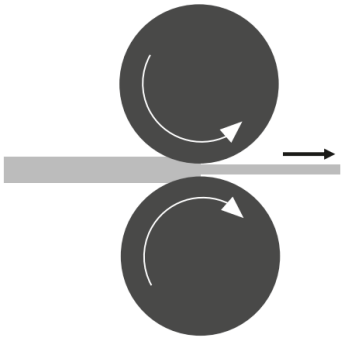

Figure 3.7: Forming through Rolling [19]

3.2.4. HOT STRIP ROLLING

As the name suggests, in hot strip rolling, the alloy or metal has to reach a temperature higher than the recrystallization phase.Hot strip is produced with a thickness of 0.8-25 mm [19]. Considering the width, narrow, medium, or wide strip can be produced. The requirements for each strip are shown in Table 3.1. In general, the process accepts cast and rolled slabs and iterates multiple times to produce hot strips. There is an option of connecting a hot rolling line directly to the casting plant, which allows low expenditure production of hot band steel from a continuous casting plant with approximately 70 mm thickness. By connecting the output process to a skin pass mill, it is possible to obtain a flat perfect strip and unify the yield points [27].As a result, a completed product, *Hot Band* is produced [12].

Type of Strip	**Width Dimension (mm)**
Narrow Strip	< 100 mm
Medium Strip	100 mm – 600 mm
Wide Strip	600 mm – 2300 mm

Table 3.1: Types of Hot Strips and Their Width Dimensions [19]

3.2.5. COLD STRIP MILL

To produce cold strip, the produced hot strip can be further processed by industrial units. For most cold rolled products, the first step is to pass the hot strip through a pickle line to eliminate impurities and rust from the metal surface [28][12]. Then, the semi-finished steel is processed through a cold rolling mill to produce steel with a thickness below 1 mm. After the cold rolling mill, the next step is to anneal the steel, which is a heat process that makes it easier to work with the metal [29][12]. It alters the physical and sometimes the chemical traits of a metal to increase its ductility and minimize the hardness. At this stage, the output material is called an annealed band, it undergoes one last process before a finished product is ready, which is the finishing mill. This process is to adjust the final product based on geometry, material and delivery condition[19]. It involves steps such as cutting, surface treatment, machining the edges, straightening and quality control sampling. The finished product is called *Cold Rolled* [12].

In general, both hot-band and cold-rolled steel serve multiple industries. One of these industries that relies on products is the automotive industry. Hot Band or Hot Rolled is used in car parts such as wheel rims and frames [30] [31]. On the other hand, Cold Rolled is used to design structural and body parts [32] [33].

4

METHODOLOGY

The methodology implemented in this paper is briefly summarized in Figure 4.1. The energy system model for the HD-R Steel process is formulated as a Mixed-Integer Linear Programming optimization problem in Python 3.11.10 solved using Gorubi [V12.0.0] on a university PC. Dashed arrows are variable while whole arrows are fixed. Unit parameters consists of batch cycle, energy consumption, maximum and minimum capacities.Material proportionalities are fixed values that determine the input and output of materials in a unit. Fuel cell and battery parameters are assumed to be installed in the plant location with a known rating. Solar and wind generation profiles are obtained from [34], [35]. A solar/wind park with a known installed capacity is assumed, but because of weather dependency, the input is variable. The energy system model accepts the above input and produces the optimal production schedule for the steel plant for a known schedule horizon. Then, a power flow analysis is conducted in PandaPower to validate the proposed network topology [36]. This is possible when the known solar and wind generation profiles are inputted into Pandapower as well. After optimization, the battery and fuel cell output within the schedule horizon are modeled as generators in PandaPower. The energy profile of all the steel units within the plant are modeled as loads, and the known solar and wind profiles are modeled as generators in Pandapower. The proposed network is validated by ensuring that the bus voltages are within acceptable limits and that the transformers are not overloaded. Then, the peak consumption of the plant (worst-case scenario) is modeled as a load on a representative European high-voltage grid.Consequently, load flow analysis is carried out to investigate how the peak consumption affects the bus voltages and line loadings on the grid.

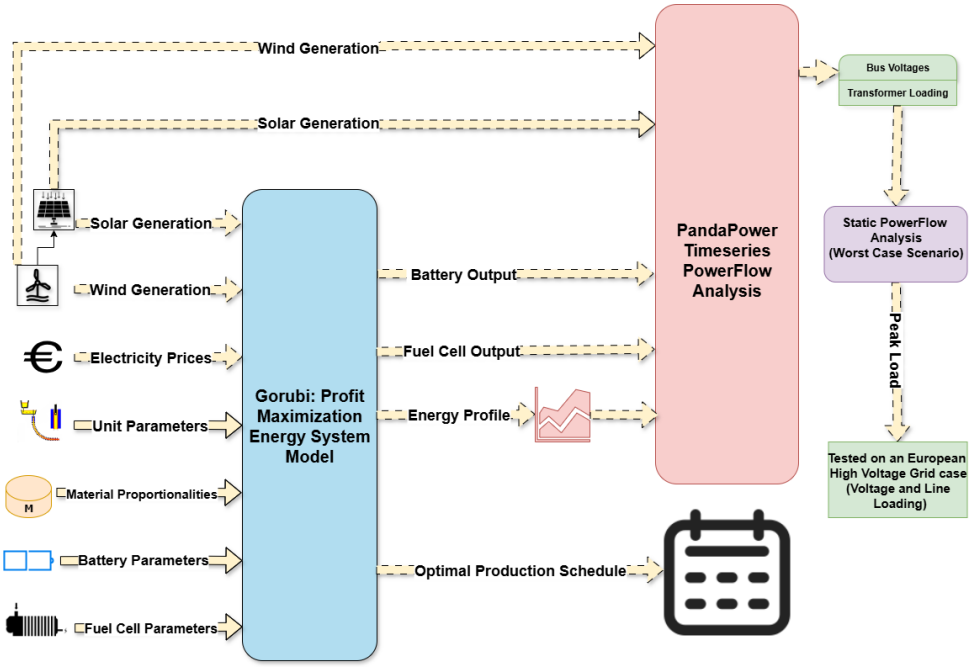

Figure 4.1: Summary of Implemented Methodology

The HD-R energy system model is created by adopting the batch-based industrial process model in [12]. This is an existing model for a steel plant operating in a batch-based process. The H_2 plant is adopted from [15] and integrated into the industrial steel model. The model is also specified for steel production by introducing more constraints related to the effects of integrating the H_2 plant. A flexibility model that is applicable to batch-based processes is introduced to highlight that grid-friendly behavior does not compromise production.

4.1. INDUSTRIAL LOADS

A steel plant operation is a batch process operation where industrial units where work collectively to produce a final product [12] ,[19]. To model the behavior of such an industrial load, its characteristics must be understood and captured accurately. To achieve this, the electrical operation for a steel plant is modeled according to the industrial smart load in [12]. This load is designed according to the following factors, peak load shaving; time-shift for the loads; pricing tariffs; renewable generation; energy storage; interruptible and uninterruptible loads; sequential operation; load dependency; size of the batch cycle; number of batch cycle for a process unit; material flow into the process unit; material balance between units; material storage; final product produced; and by-products.

4.1.1. INDUSTRIAL UNIT

An industrial unit is the building block of a plant operation that operate collectively to produce products. These units work together in a batch processing manner by consuming materials and energy to process materials further or deliver a final product. While processing, they also release energy to the environment and emissions. In figure 4.2, an industrial process is working collectively to produce materials m_8 and m_6.A unit can be represented by a rectangle or a circle, which means its uninterruptible or interruptible, respectively. Materials m_1, m_2 and m_7 are raw materials that are fed into a unit to process the materials further, they are represented by a dotted line to highlight that they can be stored at anytime. Unlike material m_5, which is represented by a bold line, because of characteristics such as temperature or pressure or other process engineering factors, material m_5 cannot be stored and has to be processed as soon as it is produced. The number inside the bracket for each unit is the time it takes to complete a batch cycle (i.e. to process input material(s) and output material(s)). For example, unit 2 requires two time slots to produce materials m_5 and m_2. Material m_3 is used as an input to units 4 and 2 which means that the units can work at the same time or not. Material m_2 is a byproduct from unit 2 that can be reused as a feed to unit 1.

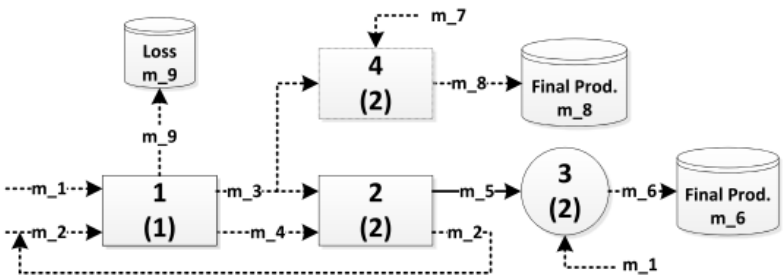

Figure 4.2: Industrial Process [12]

Without compromising quality, a unit can be broken into a small subunit to unlock new operational capabilities. For example, in figure 4.3, the unit is broken down into two sub-units 4a and 4b. If unit 4a is operational, it assumes the role of unit 4, and operates at full capacity and two time slots to produce material m_8. If unit 4b is operational, it can work at half capacity to produce material m_8 in one time-slot. The dotted line between the units highlights that they are mutually exclusive. When a unit is broken down, it is presumed that that unit can exhibit demand response by reducing its material consumption, which leads to a decrease in electricity consumption.

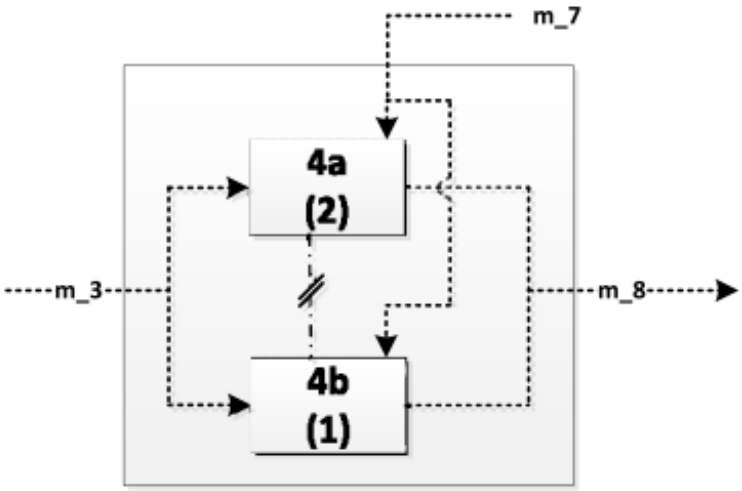

Figure 4.3: Unit 4 breakdown into smaller sub-units [12]

4.2. HYDROGEN PLANT

In [15], a preliminary Steel Making Process through Hydrogen is highlighted in Figure 4.4.This process depicts the production route of Direct Reduced Iron (DRI) or Hot Briquette Iron (HBI), which is fed into the Electric Arc Furnace (EAF). The process is comparable to the blast furnace production route, whereas in this process hydrogen is the reducing agent.

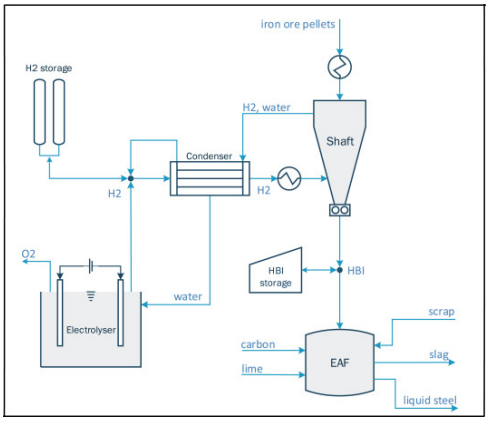

Figure 4.4: Preliminary Hydrogen Process [15]

To determine the amount of hydrogen required for the reduction process, the simplified chemical reactions in 4.3 for the preliminary hydrogen process is implemented [15].

$$H_2O_{(g)} \rightarrow H_2 + \frac{1}{2}O_2 \quad \Delta H_R = +242\,\frac{\text{kJ}}{\text{mol}} \tag{4.1}$$

$$Fe_2O_3 + 3H_2 \rightarrow 2Fe + 3H_2O_{(g)} \quad \Delta H_R = +99.5\,\frac{\text{kJ}}{\text{mol}} \tag{4.2}$$

$$Fe_2O_3 + H_2 \rightarrow 2FeO + H_2O_{(g)} \tag{4.3}$$

The reaction is endothermic which it means energy needs to be supplied to carry out the reduction. The reaction enthalpies are shown for the main reactions. The first reaction is takes place in the electrolyzer, which is the amount of energy required to breakdown the water into hydrogen and oxygen molecules. The second reaction takes place in the reduction shaft, where iron (II) oxide is reduced iron. To produce 1 ton of Direct Reduced Iron (DRI), almost 54.16 kg of Hydrogen is required. If excess hydrogen is supplied to the DR shaft, thermal requirements are minimized, which improves the efficiency of the process, which can be represented by equation 4.4 [14], [15]. Where J is the H_2 feed to shaft and Q is the amount of H_2 required to complete the reduction of iron ore.

$$\lambda = \frac{\text{J}}{\text{Q}} \quad \left[\frac{\text{mol}}{\text{mol}}\right] \tag{4.4}$$

4.3. HD-R STEEL PRODUCTION

The HD-R steel process for cold rolled and hot band steel can be seen in figure 4.4. Losses from units are stored in red blocks. Green blocks represent the storage for final products, and yellow blocks represents materials that can be used as a final product or a feed to any of the other units. Table 4.1 shows the minimum and maximum capacities and electrical energy consumption parameters for each unit. Units 1-9 are standard units that are used to produce steel, while units 10-13 are the main blocks of the hydrogen plant that is used to produce DRI. α_i and β_i represent the minimum and maximum capacity for each unit. The electricity consumption parameters c_i and d_i are in kWh/tonne and kWh, respectively. d_i is the stand-by electricity consumption for each unit.

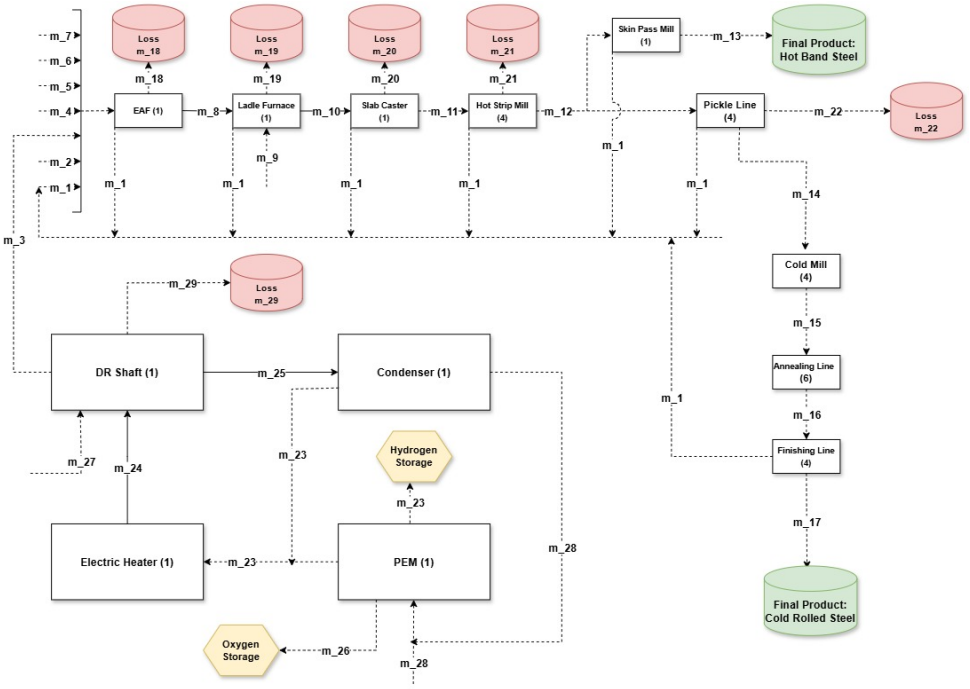

Figure 4.5: Hydrogen Reduction Steel Process Diagram

4.3.1. UNIT PARAMETERS

Energy consumption parameters for each unit assumes heat energy is electrified and part of the c_i and δ_i parameters in Table 4.1. Note that these units are not rated/sized, rather they are represented by their tonne production value and a standby electricity consumption.

i	Unit Name	α_i (tonne)	β_i (tonne)	c_i (kWh/tonne)	d_i (kWh)	References
1	Arc Furnace	10	100	494.000	24.7	[12], [13]
2	Ladle Furnace	8	80	37.500	0.278	[12]
3	Slab Caster	30	300	55.000	0.278	[12]
4	Hot Strip Mill	100	1000	284.167	0.278	[12]
5	Skin Pass Mill	4	40	13.056	0.278	[12]
6	Pickle Line	40	400	63.333	0.278	[12]
7	Cold Mill	40	400	94.444	0.278	[12]
8	Annealing Line	60	600	38.889	0.278	[12]
9	Finishing Mill	40	400	50.278	0.278	[12]
10	DR Shaft	20	100	322.000	16.1	[14], [15]
11	PEM	0.5	2,7	56760.000	1187.5	[14], [15]
12	Condenser	0.5	10	86.29	1	[14], [15]
13	Electric Heater	0.5	2.7	216.75	10	[14], [15]

Table 4.1: Parameters for Electricity Consumption for all units

4.3.2. MATERIAL PARAMETERS

Table 4.2 presents the initial amount of material at t=0, the storage capacity associated with each material in tonnes, its cost of storage (€/tonne), and the cost of consuming raw materials.Materials that cannot be stored are set to have a capacity of 0.For all scenarios, Cold Rolled (F) and Hot Band (F) are final product materials that constitute the main revenue stream.Oxygen(k=26) is a byproduct of electrolyzing water which can be used to reduce energy consumption at the Electric Arc Furnace, or as a revenue material that can be sold to combustion-based processes, fishery or the medical industry [14], [15], [37].Furthermore, Within the steel plant, oxygen can be supplied to the EAF to reduce its energy consumption. Which requires approximately 40 tonnes to reduce the energy consumption of an EAF by 22% [17]. If oxygen were to be set as a revenue material, its price can be assumed to be €60.8/t.If Oxygen was to be defined as a revenue material, its necessary to address its storage costs. Assuming liquid storage, the Levelized Cost of Liquefying Oxygen (LCOLO) is €0.04-0.334/kg. This explores the economic viability of liquefaction units and electrolyzers. In this study, the cost of storing Oxygen is assumed to be €0.04/kg since the maximum energy consumption from the PEM is around 153 MWh.With respect to water, Purification is essential to carry out electrolysis. The cost of water storage at \$0.004/H_2kg is incorporated in the the cost of storing Hydrogen [38].

k	Material Name	Initial Amount (tonnes)	Storage Capacity (tonnes)	Storage Cost (Euro/tonne)	Material Cost (Euro/tonne)	References
1	Home Scrap	10000	20000	0	0	[12]
2	Purchased Scrap	20000	20000	0	180	[12], [15]
3	Direct Reduced Iron	0	20000	276	0	[12]
4	Lime	20000	20000	0	100	[12]
5	Alloys	20000	20000	0	1777	[12], [13], [15]
6	Refractory	20000	20000	0	9.1	[12]
7	Electrode	20000	20000	0	4000	[12], [13], [15]
8	Liquid Steel	0	0	0	0	[12]
9	Carbon	20000	20000	0	10	[12], [15]
10	Treated Steel	0	0	0	0	[12]
11	Cast Steel	0	20000	0	0	[12]
12	Hot Band	0	20000	0	0	[12]
13	Hot Band (F)	0	20000	0	600	[12], [39]
14	Pickled Band	0	20000	0	0	[12]
15	Cold Rolled	0	20000	0	0	[12], [40]
16	Annealed Band	0	20000	0	0	[12]
17	Cold Rolled (F)	0	20000	0	750	[12]
18	Losses	0	20000	0	0	[12]
19	Losses	0	20000	0	0	[12]
20	Losses	0	20000	0	0	[12]
21	Losses	0	20000	0	0	[12]
22	Losses	0	20000	0	0	[12]
23	Hydrogen	0	20000	1888	0	[14], [15]
24	Heated Hydrogen	0	0	0	0	[14], [15]
25	Water Vapor	0	0	0	0	[14], [15]
26	Oxygen	0	20000	40	60.8	[14], [15], [37]
27	Iron Ore	10000	20000	0	100	[13]–[15]
28	Water	10000	20000	0	4.2	[14], [15]
29	Losses from SF	0	20000	0	0	[14]

Table 4.2: Material Storage Data including Initial Amount, Storage Capacity, and Costs

4.4. MATHEMATICAL FORMULATION

The decision variables,parameter along with the set of variables are listed in the nomenclature .

4.4.1. BATCH CYCLE'S START AND END TIME CONSTRAINTS

To keep track of the starting and ending time for a batch cycle in a unit i, constraints 4.5 and 4.6 are introduced, with $s_i[0]$=$e_i[0]$=0 as an initial condition for each unit i.

$$0 \leq s_i[t] - s_i[t-1] \leq 1, \quad \forall i, \forall t. \tag{4.5}$$

$$0 \leq e_i[t] - e_i[t-1] \leq 1, \quad \forall i, \forall t. \tag{4.6}$$

When $s_i[t]$- $s_i[t$-1] =1, a new batch cycle begins for unit i and when $e_i[t]$- $e_i[t$-1] =1, unit i finished batch cycle. To ensure that unit does not begin a new cycle when it has an ongoing cycle,constraint 4.7 must hold.

$$0 \leq s_i[t] - e_i[t-1] \leq 1, \quad \forall i, \forall t. \tag{4.7}$$

When $s_i[t]$-$e_i[t]$ =1, a unit's batch cycle is still in progress. When $s_i[t]$-$e_i[t]$ =0, the unit's batch cycle have finished before or at time t.It is also important to that all batch cycles end and do not start at the scheduling horizon T, which is ensured by constraint 4.8.

$$s_i[T] = e_i[T], \quad \forall i. \tag{4.8}$$

Consequently, the last time slot in the scheduling horizon T is used for finalizing and delivering the steel products, which means that no unit shall operate at the end of the horizon.This is enforced by constraint 4.9 is implemented.

$$x_i[T] = 0, \quad \forall i. \tag{4.9}$$

4.4.2. BATCH CYCLE'S OPERATIONAL CONSTRAINTS

Throughout the production horizon, a unit may or not operate , which is denoted by variable $x_i[t]$, which has to be related to variables $s_i[t]$ and $e_i[t]$. Therefore, let parameter a_i be the number of time slots required to complete a batch cycle for unit i. For any unit i, its batch cycle operation can be depicted using constraints 4.11 and 4.10.

$$(s_i[t] - 1)\, a_i + 1 \leq \sum_{j=1}^{t} x_i[j] \leq s_i[t] \cdot a_i, \quad \forall i, \forall t. \tag{4.10}$$

$$e_i[t] \cdot a_i \leq \sum_{j=1}^{t} x_i[j] \leq (e_i[t] + 1)\, a_i - 1, \quad \forall i, \forall t. \tag{4.11}$$

Constraints 4.10 and 4.11 ensure that when a unit is switched on at time t, it remains on for the duration of its batch cycle, while respecting the starting and ending time for a unit.

4.4.3. EXCLUSIVE OPERATION AND VARIABLE-LENGTH BATCH CYCLES CONSTRAINTS

In an industrial process, some units are mutually exclusive (i.e they cannot operate at the same time) which belong to the set X, which is depicted in constraint 4.12.

$$\sum_{i \in \mathrm{X}} \mathrm{x}_i[t] \leq 1, \quad \forall \mathrm{X}, \forall\, t. \tag{4.12}$$

Constraint 4.12 can be broken down further by considering the maximum (β_i) and minimum (α_i) capacity of a unit. Recall from Figure 4.3, when a unit is broken down into smaller units, sometimes new operations are unlocked.To enable a variable-length batch cycle for unit i, constraint 4.12 is applied to unit 4, which is shown in inequality 4.13.

$$\mathrm{x}_{4\mathrm{a}}[t] + \mathrm{x}_{4\mathrm{b}}[t] \leq 1, \quad \forall\, t. \tag{4.13}$$

To elaborate further, when unit 4a is operating, its the same as unit 4 is operating (α_4, β_4, and a_4 remain the same). When unit 4b is On, α_4, β_4, and a_4 are halved. This relationship is can described using equation 4.14.

$$\beta_{4\mathrm{a}} = \beta_4, \quad \beta_{4\mathrm{b}} = 1/2\,\beta_4, \quad \mathrm{a}_{4\mathrm{a}} = \mathrm{a}_4, \quad \mathrm{a}_{4\mathrm{b}} = 1/2\,\mathrm{a}_4. \tag{4.14}$$

4.4.4. INPUT AND OUTPUT TIMING CONSTRAINTS

A unit may accept material if and only if it begins its batch cycle. In addition, it can only output material if and only if its batch cycle has ended. It was previously mentioned that a unit begins a new batch cycle only when $\mathrm{s}_i[t]$-$\mathrm{s}_i[t-1] = 1$ and finishes a batch only when $\mathrm{e}_i[t]$-$\mathrm{e}_i[t-1] = 1$. Accordingly, constraints 4.15 and 4.16 are implemented to comply with the input timing when a unit begins a new batch cycle and output timing when it finishes its batch cycle. It also incorporates maximum and minimum capacity to ensure that for unit capacities are not breached.

$$\mathrm{u}_i[t] \geq (\mathrm{s}_i[t] - \mathrm{s}_i[t-1])\,\beta_i, \quad \forall\, i, \forall\, t. \tag{4.15}$$

$$\mathrm{u}_i[t] \leq (\mathrm{s}_i[t] - \mathrm{s}_i[t-1])\,\alpha_i, \quad \forall\, i, \forall\, t. \tag{4.16}$$

Furthermore, to satisfy the right timing of output for any unit i, constraints 4.17 and 4.18 are adopted, where Ω_{cap} is a number that should be greater than the largest maximum capacity (β_i) of all units.

$$\mathrm{y}_i[t+1] \geq 0, \quad \forall\, i, \forall\, t < T. \tag{4.17}$$

$$\mathrm{y}_i[t+1] \leq \Omega_{\mathrm{cap}}\,(\mathrm{e}_i[t] - \mathrm{e}_i[t-1]), \quad \forall\, i, \forall\, t < T. \tag{4.18}$$

It is also important that any unit i does not produce material at the beginning of the scheduling horizon,i.e at time slot t=1. Which is represented in constraint 4.19.

$$\mathrm{y}_i[1] = 0, \quad \forall\, i. \tag{4.19}$$

4.4.5. MATERIAL BALANCE AND PROPORTIONALITY CONSTRAINTS

In general, material balance means that the amount of material entering a unit i must be equal to the amount of material that leaves a unit i in a batch cycle. This also includes the losses when materials are processed. It should stand for a unit i , and among all units in the plant. Constraint 4.20 ensures that the total amount of material that enters a unit i is equivalent to the total amount of material that leaves unit i.

$$0 \leq \sum_{j=1}^{t} \mathrm{u}_i[j] - \sum_{j=1}^{t} \mathrm{y}_i[j+1] \leq \Omega\,(1 - \mathrm{e}_i[t] + \mathrm{e}_i[t-1]), \quad \forall\, i, \forall\, t < T. \tag{4.20}$$

To ensure that material balance is valid across all the units, constraint 4.21 must hold.

$$\mathrm{m}_k[t] = \mathrm{m}_k[t-1] + \sum_{i \in I_k^{\mathrm{out}}} \mathrm{q}_i^k\, \mathrm{y}_i[t] - \sum_{i \in I_k^{\mathrm{in}}} \mathrm{r}_i^k\, \mathrm{u}_i[t], \quad \forall\, k, \forall\, t. \tag{4.21}$$

Constraint 4.21 is applicable to all materials, whether they can be stored or not. Varaible $m_k[0]$ is initial amount of storage for all materials k at the beginning of the production process. In the second expression, $q_i^k y_i[t]$ is the proportionality of material k that is produced from the set of units I_k^{out} that output material k. Similarly, r_i^k is the proportionality of material k that is fed into the set of units I_k^{in} that output material k. It is important to note that for each unit i, $\sum_{k \in \mathcal{K}} \mathrm{r}_i^k = 1$ and $\sum_{k \in \mathcal{K}} \mathrm{q}_i^k = 1$.

4.4.6. MATERIAL STORAGE

For any material k that can be stored, its maximum capacity cannot be exceeded. Accordingly, constraint 4.22 is implemented to ensure that storage capacities are not voided. Where η_k is the maximum storage capacity for material k.

$$0 \leq \mathrm{m}_k[t] \leq \eta_k, \quad \forall\, k,\ \forall\, t. \tag{4.22}$$

Previously, it was mentioned that some materials cannot be stored and have to be processed immediately. As a result, constraint 4.23 is introduced to address such materials that belong to set $\mathcal{K}_{\mathrm{imd}}$.

$$\eta_k = 0, \quad \forall\, k \in \mathcal{K}_{\mathrm{imd}}. \tag{4.23}$$

Finally, to set a production requirement such that final products are produced at the end of the scheduling horizon (T), constraint 4.24 is implemented. Where ϕ_f is the minimum production requirement and $\mathcal{F}$ is the set of materials are final products.

$$\mathrm{m}_f[\mathrm{T}] \geq \phi_{\mathrm{f}}, \quad \forall\, f \in \mathcal{F}. \tag{4.24}$$

4.4.7. UNINTERRUPTIBLE UNITS CONSTRAINT

As mentioned in section 4.1.1, the operation of units that are represented by a rectangle cannot be stopped once their batch cycle has started, while a circled unit's operation can interrupted and resumed at a later time. Since a unit's batch cycle can only start if

and only if s_i[t]-s_i[t-1] =1, it should ensure that x_i[t]=x_i[t+1]=...x_i[t+a_i-1]=1 for all uninterruptible units. Additionally, this constraint should be bounded between t=1 and t=T-a_i+1 such that all batch cycles finish before the scheduling horizon. The mathematical representation for this constraint is in equation 4.25.

$$s_i[t] - s_i[t-1] \leq x_i[t+j], \quad \forall\, i \in \mathscr{I}_{\text{unt}},\ \forall\, t \in [1, T-j]. \tag{4.25}$$

Where j=0,1,2,...$a_i - 1$ for all uninterruptible units.

4.4.8. ELECTRICITY CONSUMPTION CONSTRAINT:UNIT

The electricity consumption of a unit depends on the amount of material it processes in a batch cycle. Any unit i consumes raw or semi-processed material(s) and produces semi-processed or output material (s), as shown in equation 4.26.

$$M_i[t] = \sum_{j=1}^{t} u_i[j] - \sum_{j=1}^{t} y_i[j], \quad \forall\, i \quad \forall\, t. \tag{4.26}$$

Relating the equation 4.26 to electricity consumption, constraints 4.27 and 4.28 are introduced, where parameter c_i is an electricity consumption parameter that is in [kWh/tonne], and parameter d_i is a standby electricity consumption parameter in [kWh], it represents the standby electricity consumption for all parameters.In this constraint, Ω_i is a large enough number that is selected to be slightly greater than the value of the greatest product between the maximum capacity of a unit and its electricity consumption parameters. Mathematically, when $x_i[t] = 0$, Ω_{ele} has to be larger than the term $c_i\, M_i[t] + d_i$ to activate constraint 4.27. When $x_i[t] = 1$, constraint 4.28 is activated and the energy consumption of a unit depends on the amount of material that is processed in its batch cycle.

$$l_i[t] \geq d_i, \quad \forall\, i,\ \forall\, t \tag{4.27}$$

$$l_i[t] \geq c_i \cdot M_i[t] + d_i - \Omega_{\text{ele}} \cdot (1 - x_i[t]), \quad \forall\, i,\ \forall\, t. \tag{4.28}$$

4.4.9. ELECTRICITY CONSUMPTION CONSTRAINT:PLANT

Equation 4.29 is the demand profile of the plant operation, which is represented by the summation of the electricity consumption for all units at time t and the background load ($l_{back}[t]$) of the plant. The background load represents lighting, sockets, office loads... etc.

$$L[t] = \sum_{i \in \mathscr{V}} l_i[t] + l_{\text{back}}[t], \quad \forall\, t. \tag{4.29}$$

Equation 4.29 can be reformulated to include an industrial battery ($l_{ch}[t]$ & $l_{dch}[t]$), renewable on-site generation ($l_{Re}[t]$), and a fuel cell($l_{fc}[t]$) as shown in equation 4.30. The subsequent sections explain the origin of these variables.

$$L[t] = \sum_{i \in \mathscr{V}} l_i[t] + l_{\text{back}}[t] - l_{\text{RE}}[t] - l_{\text{dch}}[t] - l_{\text{fc}}[t] + l_{\text{ch}}[t], \quad \forall\, t. \tag{4.30}$$

Furthermore, at any time t, the plant consumption should not exceed the maximum grid connection imposed by the grid operator. This is ensured by constraint 4.31.

$$L[t] \leq L_{max}, \quad \forall\, t. \tag{4.31}$$

4.4.10. ELECTRICITY CONSUMPTION CONSTRAINT:RENEWABLE GENERATION

$l_{Re}[t]$ is the summation of the solar $l_{solar}[t]$ and wind generation $l_{wind}[t]$ at time t as shown in equation 4.32.

$$l_{RE}[t] = l_{solar}[t] + l_{wind}[t] \tag{4.32}$$

4.4.11. ELECTRICITY CONSUMPTION CONSTRAINT:INDUSTRIAL BATTERY

$l_{ch}[t]$ and $l_{dch}[t]$ are decision variables that represent the charging and discharging rate for the industrial battery at any time t, respectfully. To ensure that charging and discharging does not occur simultaneously, constraints 4.33 and 4.34 are introduced. Where $b[t]$ is a binary decision variable that indicates whether a battery is charging or discharging, if $b[t] = 1$, it charging up to it maximum charging capacity (l_{ch}^{max}). If $b[t] = 0$, the battery is discharging up to its maximum discharging capacity (l_{dch}^{max}).

$$0 \leq l_{ch}[t] \leq b[t] \cdot l_{ch}^{max}, \quad \forall\, t. \tag{4.33}$$

$$0 \leq l_{dch}[t] \leq (1 - b[t]) \cdot l_{dch}^{max}, \quad \forall\, t. \tag{4.34}$$

Furthermore, charging cannot take place when the battery is full and the battery cannot discharge when its empty. Accordingly, constraint 4.35 is implemented where μ and θ are the charging and discharging efficiencies, respectfully. B^{full} is full charge capacity and B^{init} is the initial battery capacity.

$$0 \leq B^{init} + \sum_{j=1}^{t} \left(\mu \cdot l_{ch}[j] - \theta \cdot l_{dch}[j]\right) \leq B^{full}, \quad \forall\, t. \tag{4.35}$$

4.4.12. ELECTRICITY CONSUMPTION CONSTRAINT:FUEL CELL

In a fuel cell,Hydrogen and Oxygen react to produce electricity and water. This means that the material proportionality constraint 4.21 should be specified for Hydrogen, Oxygen and water. Constraints 4.36, 4.37 and 4.38 capture the material consumption and production for a fuel cell. Where $m_{H2\text{-}FC}[t]$ is a decision variable that tracks the amount of Hydrogen used to generate electricity at any time t. In constraint 4.37, the term $8 \cdot m_{H2\text{-}FC}$ is the amount of oxygen used in a fuel cell in terms of hydrogen consumption, which needs to be subtracted from the oxygen storage. The same is applicable to the water produced from the cell in constraint 4.38, the term $9 \cdot m_{H2\text{-}FC}$ is the amount of water produced in a fuel cell in terms of hydrogen consumption that is circulated back to storage. The values 8 and 9 can be verified by means of stoichiometric calculations for the fuel cell reaction. It is assumed that the water circled back to storage does not require any purification.

$$m_{H2}[t] = m_{H2}[t-1] + \sum_{i \in I^{out}_{H2}} q^{H2}_i \cdot y_i[t] - \sum_{i \in I^{in}_{H2}} r^{H2}_i \cdot u_i[t] - m_{H2\text{-}FC}[t], \quad \forall\, t \tag{4.36}$$

$$m_{O2}[t] = m_{O2}[t-1] + \sum_{i \in I^{out}_{O2}} q^{O2}_i \cdot y_i[t] - \sum_{i \in I^{in}_{O2}} r^{O2}_i \cdot u_i[t] - 8 \cdot m_{H2\text{-}FC}[t], \quad \forall\, t \tag{4.37}$$

$$m_{H2O}[t] = m_{H2O}[t-1] + \sum_{i \in I^{out}_{H2O}} q^{H2O}_i \cdot y_i[t] - \sum_{i \in I^{in}_{H2O}} r^{H2O}_i \cdot u_i[t] + 9 \cdot m_{H2\text{-}FC}[t], \quad \forall\, t \tag{4.38}$$

The generated electricity ($l_{FC}[t]$) from a fuel cell can be calculated by using equation 4.39. Where HHV_{H2} is the Higher Heating Value of Hydrogen and FC^{eff} is the fuel cell efficiency. Since Hydrogen is the energy content reactant and needs Oxygen to produce electricity, it is assumed that oxygen is not a limiting reactant in the fuel cell operation.

$$l_{FC}[t] = m_{H2\text{-}FC}[t] \cdot HHV_{H2} \cdot FC^{eff}, \quad \forall\, t. \tag{4.39}$$

4.4.13. ELECTRICITY CONSUMPTION CONSTRAINT:OXYGEN

Oxygen can be used to reduce the energy consumption for combustion based units such as the EAF. For 40 tonnes of oxygen supply, the energy consumption of the EAF can be reduced by 22% [17]. The energy parameters of the EAF in this model has a maximum consumption of 49424.7 kWh when its fully loaded [12]. Consuming 40 tonnes of oxygen reduces the energy consumption by 9884.4 kWh, which is equivalent to 247.1235 kWh for each tonne Oxygen. The constant 247.1235[kWh] is referred to as O. Therefore, a new decision variable $m_{O2\text{-}EAF}[t]$ tracks the oxygen consumption for the EAF. Note that the term $x_1[t]$ is the operational binary decision variable for the Electric Arc Furnace, oxygen consumption should not be triggered while the unit is on standby-mode.The constraint 4.37 is reformulated to incorporate oxygen consumption in the EAF in the constraint 4.40.

$$\begin{aligned} m_{O2}[t] = m_{O2}[t-1] &+ \sum_{EAF \in I^{out}_{O2}} q^{O2}_{EAF} \cdot y_{EAF}[t] \\ &- \sum_{EAF \in I^{in}_{O2}} r^{O2}_{EAF} \cdot u_{EAF}[t] - 8 \cdot m_{H2\text{-}FC}[t] - x_{EAF}[t] \cdot m_{O2\text{-}EAF}[t], \quad \forall\, t. \end{aligned} \tag{4.40}$$

The amount of energy saved by oxygen supply ($l_{EAF\text{-}O2}[t]$) at any time t can be simply calculated using equation 4.41.Furthermore, At any time t , the consumption of oxygen at the EAF cannot exceed 40 tonnes, which is depicted in constraint 4.42.

$$l_{EAF\text{-}O2}[t] = m_{O2\text{-}EAF}[t] \cdot O, \quad \forall\, t. \tag{4.41}$$

$$m_{O2\text{-}EAF}[t] \leq 40, \quad \forall\, t. \tag{4.42}$$

To consider the energy reduction for the EAF, $l_{\text{EAF-O2}}$ has to be reflected at the energy consumption of the EAF. Therefore, constraint 4.28 is further detailed for unit 1(i.e EAF) as shown in constraint **??**.

$$l_i[t] - l_{\text{EAF-O2}}[t] \geq c_i \cdot M_i[t] + d_i - \Omega_{\text{ele}} \cdot (1 - x_i[t]), \quad \forall\, t. \tag{4.43}$$

4.4.14. OBJECTIVE FUNCTION

Usually, steel manufacturers set their objective function to maximize their production [10]. By adopting this approach, steel owners risk exploring other revenue streams.Therefore, a profit-maximization objective function is optimized in this model is equation 4.44. The revenues are the final products sold at a given price and the amount of energy saved from flexible operation. Costs include storage costs for any material k,cost of consuming raw materials, fixed costs and variable costs from electricity consumption.

$$\max \sum_{f \in \mathscr{F}} m_f[T]\, p_f - \sum_{r \in \mathscr{R}} (m_r[0] - m_r[T])\, p_r - \sum_{t=1}^{T} \sum_{k \in \mathscr{K}} m_k[t]\, \gamma_k - C_{\text{fixed}} - C_{\text{ele}} - C_{\text{labour}} - C_{\text{CO2}} \tag{4.44}$$

Where γ_k is the cost of storing a material and C_{fixed} are fixed costs that are used in manpower, operation and maintenance.. etc. C_{labour} is the cost of producing one tonne of liquid steel. The cost of electricity C_{ele} is calculated based on the electricity consumption of the plant. Which is defined in equation 4.45, where $L[t]$ is the total electrical energy consumption of the plant at a time slot t. The wholesale electricity price is $p[t]$ and the cost is summed over the scheduling Horizon T. $\mathscr{F}$ is the set of final products sold to generate revenue and $\mathscr{R}$ is the set of raw materials that are consumed in the production schedule.

$$C_{\text{ele}} = \sum_{t=1}^{T} L[t]\, p[t] \tag{4.45}$$

The cost of producing carbon is calculated using equation 4.46. Where p_{CO2} is the fixed price of emitting carbon. The term $\mathscr{C}$ is the set of materials k that emit CO_2. The summation term represents the sum of all materials that are consumed over the scheduling horizon T and emit CO_2.It is assumed that half of these materials are processed and other half react with oxygen to produce CO_2 [15].

$$C_{\text{CO2}} = p_{\text{CO2}} \cdot 0.5 \cdot \sum_{k \in \mathscr{C}} (m_k[0] - m_k[T]) \tag{4.46}$$

4.4.15. FLEXIBILITY

Units that can reduce their electricity consumption without compromising production requirements are known as flexible units and belong to

A flexible unit is a unit the has the option to reduce its electricity consumption by selling the reduced volume back to the market or resume normal operation as per scheduling requirements. F. Such units have the option to schedule normal operation or an operation with reduced electrical energy consumption where the reduced volume is sold

back to the electricity market. To clarify, the sold electricity is not physically sent back to the grid, rather it is a market transaction that takes place before the units process material(s). The total volume of reduced energy for all the flexible units can be calculated using equation 4.47.It should also be noted that there are multiple markets in the Netherlands which can accept the offered capacity, which can open further revenue streams.

$$\mathrm{L_{flex}}[t] \;=\; \sum_{i \in F} \mathrm{w}_i[t]\,\mathrm{c}_i, \qquad \forall\, t. \tag{4.47}$$

Where $L_{flex}[t]$ is the total amount of energy offered by the flexible units at time t. $w_i[t]$ is a decision variable that represents the amount of mass that can be offered by any flexible unit i at time t in [tonnes], and $c_i[t]$ is the same as previously defined which is the parameter of electricity consumption for any unit i in [kWh/tonnes]. To incentivize the units to offer electricity consumption, the objective function is re-formulated when the model is operating in a flexible manner. The objective function in equation 4.44 becomes the profit maximization function including flexibility in equation 4.48.

$$\max \sum_{f \in \mathscr{F}} \mathrm{m}_f[T]\,\mathrm{p}_f + \sum_{t=1}^{T} \mathrm{R_{flex}}[t] - \sum_{r \in \mathscr{R}} (\mathrm{m}_r[0] - \mathrm{m}_r[T])\,\mathrm{p}_r - \sum_{t=1}^{T} \sum_{k \in \mathscr{K}} \mathrm{m}_k[t]\,\gamma_k - \mathrm{C_{fixed}} - \mathrm{C_{ele}} - \mathrm{C_{labour}} - \mathrm{C_{CO2}} \tag{4.48}$$

Where $R_{flex}[t]$ is the revenue earned by the industrial consumer as a result of flexible volume offered by the units. It is expressed in equation 4.49, where $p[t]$ is the wholesale electricity price at time t.

$$\mathrm{R_{flex}}[t] \;=\; \mathrm{L_{flex}}[t]\,\mathrm{p}[t], \qquad \forall\, t. \tag{4.49}$$

It is important to note that decision variable $w_i[t]$ only impacts the material input for a unit. The difference between $u_i[t]$ and $w_i[t]$ is the actual amount of material that enters a unit. Therefore, when the model is operating in flexible mode, the following operational constraints must take into account decision variable $w_i[t]$ .Equation 4.26 determines the amount of material that processed in a batch cycle in unit i fo its electricity consumption. It is re-formulated to consider $w_i[t]$ in equation 4.50.

$$\mathrm{M_i[t]} = \sum_{\mathrm{j=1}}^{\mathrm{t}} \mathrm{u_i[j]} - \sum_{\mathrm{j=1}}^{\mathrm{t}} \mathrm{y_i[j]} - \sum_{\mathrm{j=1}}^{\mathrm{t}} \mathrm{w_i[j]}, \quad \mathrm{i} \in F,\ \forall\, \mathrm{t} \tag{4.50}$$

Equation 4.50 only accounts for material processed in a batch cycle for electricity consumption. Therefore, constraints 4.15,v 4.16 have to adjust to decision variable $w_i[t]$ the amount of material entering a unit is still bounded by its minimum and maximum capacities.Accordingly, this is reflected in constraints 4.51 and 4.52.

$$\mathrm{u}_i[t] - \mathrm{w}_i[t] \geq (\mathrm{s}_i[t] - \mathrm{s}_i[t-1])\,\alpha_i, \quad \forall\, i \in F,\ \forall\, t. \tag{4.51}$$

$$\mathrm{u}_i[t] - \mathrm{w}_i[t] \leq (\mathrm{s}_i[t] - \mathrm{s}_i[t-1])\,\beta_i, \quad \forall\, i \in F,\ \forall\, t. \tag{4.52}$$

Furthermore, to ensure that material balance still holds across all units, constraint 4.20 is re-formulated as constraint 4.53. In this manner, when a unit completes its batch

cycle, the actual amount of material that enters a unit i is the difference between $u_i[t]$and $w_i[t]$ equivalent to $y_i[t]$, the amount of material that leaves a unit i.

$$0 \leq \sum_{j=1}^{t} u_i[j] - \sum_{j=1}^{t} w_i[j] - \sum_{j=1}^{t} y_i[j+1] \leq \Omega\,(1 - e_i[t] + e_i[t-1]), \quad \forall\, i \in F,\ \forall\, t < T. \tag{4.53}$$

By considering the re-formulated constraints 4.50, 4.51, 4.52 and 4.53, the model can now demonstrate flexible mode and respect the operational constraints in smart control mode. However, decision variable $w_i[t]$ must be bounded by realistic assumptions that reflect the nature of the model.At t=T, all the units are switched off and are used to deliver final products. Therefore, no electricity volume should be offered to the electricity market. This is seen in constraint 4.54.

$$w_i[T] = T, \quad \forall\, i \in F. \tag{4.54}$$

$$w_i[T] = 0, \quad \forall\, i \in F. \tag{4.55}$$

At t=0, units are also switched off since its the beginning of the schedule horizon. Constraint 4.55 enforces this behavior.

$$w_i[0] = 0, \quad \forall\, i \in F. \tag{4.56}$$

Finally, the actual reduction in the unit input cannot exceed the maximum capacity of the unit. Therefore, constraint 4.57 is introduced to maintain the input unit loading within the capacity for any unit i.

$$w_i[t] \leq \beta_i\, \epsilon, \quad \forall\, i \in F,\ \forall\, t. \tag{4.57}$$

Where ϵ is a continuous parameter that sets the maximum material capacity that can be reduced by any unit i. Its maximum value is 1 and will later be used to conduct sensitivity analysis.

4.5. MODELING ASSUMPTIONS

4.5.1. PROPORTIONALITY OF MATERIALS

In some cases, the proportionality of material that enters or leaves a unit is not directly available from open literature.In such cases, the proportionality of materials entering a unit is calculated using equations 4.58. where $U_{k,i}$ is the amount of material k that is entering a unit i, and Y_i is the total amount of material that enters unit i.When material leaves a unit, equation 4.59 is used to calculate the proportionality of output for material k that leaves a unit i. Where $A_{k,i}$ is the amount of material k that leaves a unit i and N_i is the total amount of material that leaves a unit i.For Units 1-9, these values are obtained from [12]. For units 10-13, the values are calculated using equation 4.58. The calculated proportionalities for every material that leaves or enters a unit is in appendix **??**.

$$r_i^k = \frac{U_{k,i}}{Y_i} \tag{4.58}$$

Table 4.3: Input and Output Proportionality of Materials for All Units

Unit Name	Material Input	Proportion	Material Output	Proportion
Unit 1: Electric Arc Furnace	Home Scrap	0.125	Liquid Steel	0.79
	Purchased Scrap	0.376		
	DRI	0.442		
	Lime	0.036	Home Scrap	0.02
	Alloys	0.005		
	Refractory	0.014	Losses	0.19
	Electrode	0.002		
Unit 2: Ladle Furnace	Carbon	0.0004	Treated Steel	0.965
	Liquid Steel	0.9996	Home Scrap	0.021
			Losses	0.014
Unit 3: Slab Caster	Treated Steel	1	Cast Steel	0.965
			Home Scrap	0.049
			Losses	0.01
Unit 4: Hot Strip Mill	Cast Steel	1	Hot Band	0.965
			Home Scrap	0.025
			Losses	0.01
Unit 5: Skin Pass Mill	Hot Band	1	Home Scrap	0.01
			Hot Band (F)	0.99
Unit 6: Pickle Line	Hot Band	1	Pickled Band	0.99
			Home Scrap	0.01
Unit 7: Cold Mill	Pickled Band	1	Cold Rolled	1
Unit 8: Annealing Line	Cold Rolled	1	Annealed Band	1
Unit 9: Finishing Mill	Annealed Band	1	Home Scrap	0.05
			Cold Rolled (F)	0.95
Unit 10: DR Shaft	Iron Ore	0.962	Water Vapor	0.3105
	Heated Hydrogen	0.038	Direct Reduced Iron	0.68911
			Losses from SF	0.00039
Unit 11: PEM	Water	1	Oxygen	0.89
			Hydrogen	0.11
Unit 12: Condenser	Water Vapour	1	Hydrogen	0.001
			Water	0.999
Unit 13: Electric Heater	Hydrogen	1	Heated Hydrogen	1

$$\mathrm{q}_i^k = \frac{\mathrm{A}_{k,i}}{\mathrm{N}_i} \tag{4.59}$$

4.5.2. BATTERY AND FUEL CELL PARAMETERS

BATTERY

An industrial battery with parameters in Table 4.4 is introduced as a form of short-term energy storage [12].

Table 4.4: Battery Parameters

Parameter	Description	Value
B_{initial}	Initial battery energy [kWh]	1500
B_{full}	Battery capacity [kWh]	5000
$\ell^{\text{ch}}_{\text{max}}$	Maximum charging power [kW]	2500
$\ell^{\text{dch}}_{\text{max}}$	Maximum discharging power [kW]	2500
μ	Charging efficiency [-]	0.95
θ	Discharging efficiency [-]	0.90

4.5.3. FUEL CELL

Mainly, Hydrogen production is intended for reducing Iron (II) Oxide. However, given its energy storage qualities, a fuel cell may operate to reduce the energy consumption of the plant. The parameters of the fuel cell is in Table 4.5.

Table 4.5: Fuel Cell Parameters

Parameter	Description	Value
ℓ^{fc}_{max}	Maximum fuel cell output [kWh]	50
E^{HHV}_{H2}	Hydrogen energy content (HHV) [kWh/kg]	33.3
η_{fc}	Fuel cell efficiency	0.60

4.5.4. PRICE PROFILE

If steel consumer were to procure electricity from the market, a 48h price profile is selected as input for $p_{ele}[t]$ is selected from the Day-Ahead market in the Netherlands in the year 2023.Three price profile will be selected from that period. The first profile will contain peak prices relative to the yearly profile, while the second profile is low price. In case of a fixed price scenario, its assumed that the steel consumer secured a bi-lateral contract from a generation company. In that case, p_{ele} is the average of the Day-Ahead price of electricity in the Netherlands in 2023, which is 0.097 €/MWh [41]. Price profiles are obtained from the Day-Ahead Market in 2023 in the Netherlands [42].Three profiles are selected, they represent scenarios where prices low, average and peak prices. Figures 4.6,4.7, and 4.8 show the profiles for peak,average and low prices, respectively.

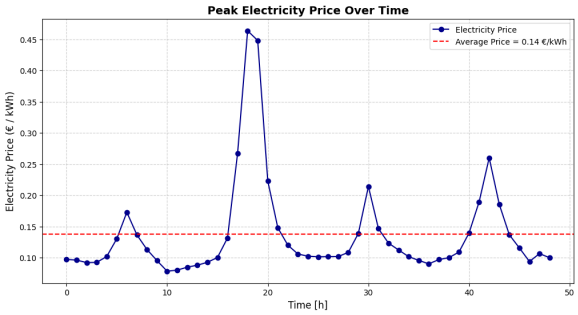

Figure 4.6: Electricity price profile under peak pricing conditions.

C_{fixed} is selected to be zero, the cost of emitting carbon C_{CO_2} is assumed to be €86.68/tCO_2, and the labor cost is is €53.2/tLS [15],which considers the hydrogen plant, DR Shaft and the EAF without assuming downstream units.

4.5.5. MATERIAL DATA

Unless stated otherwise,the minimum production requirement is selected to be 100 tonnes for Hot Band (F) and 700 tonnes for Cold Rolled (F) through constraint 4.24. The is production requirement is applicable to all scenarios except when flexibility is considered.

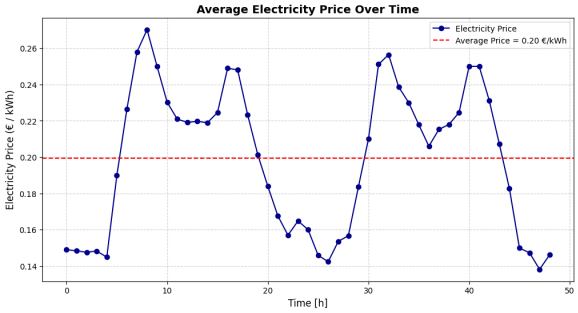

Figure 4.7: Electricity price profile under average pricing conditions.

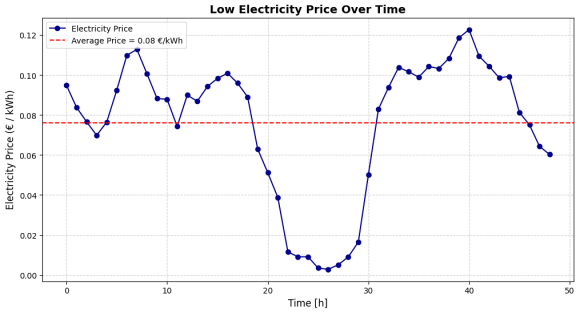

Figure 4.8: Electricity price profile under low pricing conditions.

Oxygen(k=26) is a byproduct of electrolyzing water which can be used to reduce energy consumption at the Electric Arc Furnace, or as a revenue material that can be sold to combustion-based processes, fishery or the medical industry [14], [15], [37].It can also be supplied to the EAF to reduce its energy consumption. Which requires approximately 40 tonnes to reduce the energy consumption of an EAF by 22% [17]. If oxygen were to be set as a revenue material, its price can be assumed to be €60.8/t.If Oxygen was to be defined as a revenue material, its necessary to address its storage costs. Assuming liquid storage, the Levelized Cost of Liquefying Oxygen (LCOLO) is €0.04-0.334/kg and is assumed to be [37] €0.04/kg in this study. Water is also stored and requires purification for electrolysis, which has an a storage cost at \$0.004/H_2kg [38].

4.5.6. RENEWABLE GENERATION

The solar and wind energy profiles are obtained from Renwableninja with a capacity of 1 MW Delft, Netherlands[34], [35]. Since there are three prices profiles that each correspond to different time periods, the solar and wind profiles will based for each of these time periods. Figures 4.10, 4.9, 4.11 show the solar, wind and total renewable generation for the peak, average and low price durations,respectively.

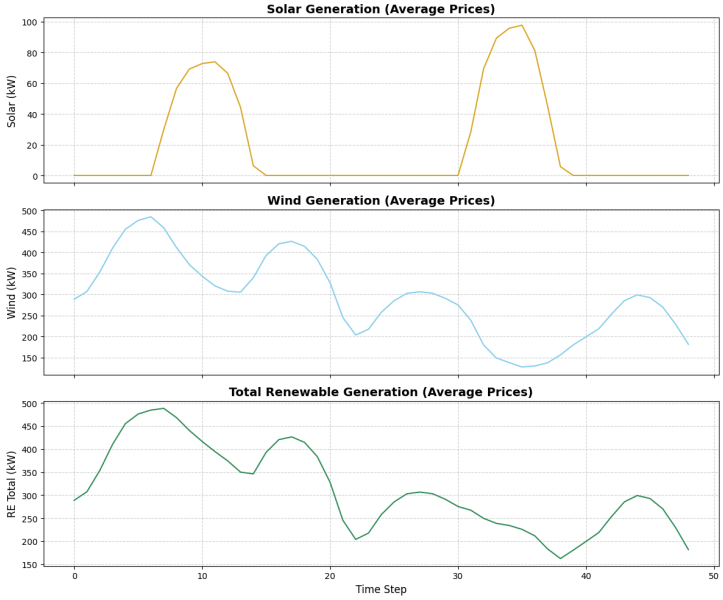

Figure 4.9: Renewable generation profiles (Solar, Wind, Total) during average price periods.

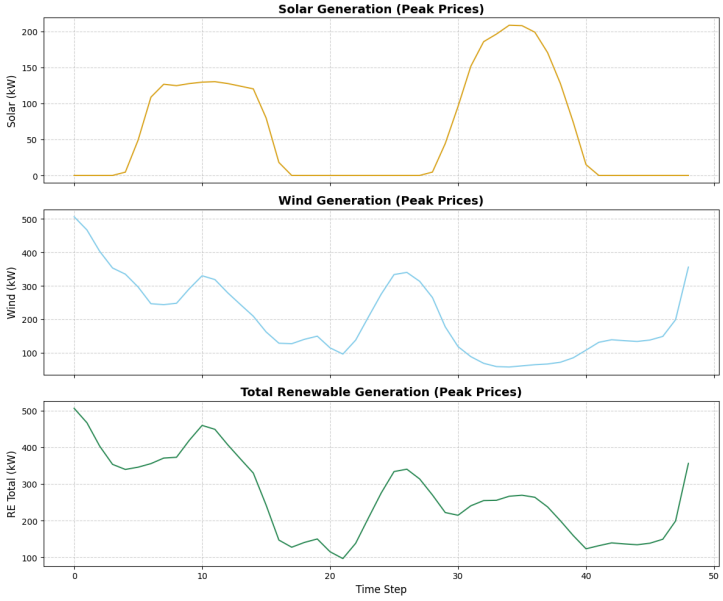

Figure 4.10: Renewable generation profiles (Solar, Wind, Total) during peak price periods.

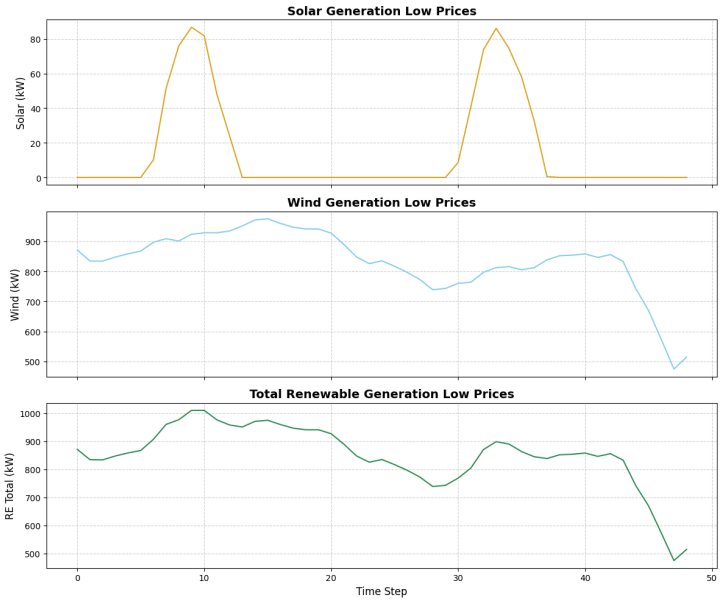

Figure 4.11: Renewable generation profiles (Solar, Wind, Total) during low price periods.

4.5.7. HYDROGEN STORAGE

The cost of Hydrogen storage depends on the technology and the location. Common technologies for Hydrogen storage are line packing, salt caverns, pressurized and liquid cryogenic storage.The capacities and duration of the each technology can be found in Table 4.6. All technologies besides salt caverns, are independent of their location. Accordingly, the model adopts a large scale liquid cryogenic storage at 10 tonnes with a cost of storage at €1.88/$H2$kg (in addition to cost of storing purified water at €0.04/$H2$kg , which is translated to tonnes in the model [43].

Table 4.6: Hydrogen storage technologies by typical duration and capacity [43]

Storage Technology	**Typical Duration of Storage**	**Tonnes of H_2 Typically Stored**
Line packing	1 day or less	100–300
Salt cavern	2–4 months	500–1000
Above ground pressurized tank (GH_2)	1–2 days	0.3–1.0
Above ground liquid tank (LH_2)	1–2 weeks	5–10

4.5.8. SET OF FLEXIBLE UNITS

Unlocking the potential for flexibility involves a deeper understanding of the electrical behavior and industrial traits of each unit.Table 4.7 shows which units can assume flexible operation throughout the production horizon. The reasons for the assumptions are

highlighted as follows for each unit. Units such as EAF, LF,Slab Caster, Electric Heater, DR Shaft, and the Condenser interact with materials that cannot be stored.Therefore, they are not considered in the set of flexible units, as they could potentially severely affect the production requirements. The PEM is known to be robust against degradation because of its switching capabilities [44], which makes it suitable for flexible operation. The Hot Strip Mill offers high potential for flexible operation because of its capacity and energy intensity. However, this comes with a greater risk of delaying the steel production line[11]. Units such as Skin Pass Mill, Pickle Line, Cold Mill, Annealing Line and Finishing Line are part of the impurity and further product detailing units, which are all assumed to be part of the set of flexible units.

Table 4.7: Unit Flexibility of Process Units in an HD-R Steel Process

Unit	Flexible Operation
Electric Arc Furnace (EAF)	No
Ladle Furnace (LF)	No
Hot Strip Mill	No
Slab Caster	No
Skin Pass Mill	Yes
Pickle Line	Yes
Cold Mill	Yes
Annealing Line	Yes
Finishing Mill	Yes
Electrolyzer	Yes
Electric Heater	No
Direct Reduction Shaft	No
Condenser	No

4.6. POWER SYSTEM MODELING

Power flow (or load flow) analysis is a fundamental tool in power system engineering. Its objective is to determine the steady-state operating conditions of an electrical network, specifically the distribution of active and reactive power flows, voltages, and currents. The information is essential to ensure safe operation by respecting voltage and current limits, verifying supply-demand balance, and detecting line overloads. AC Powerflow is the default pandapower load flow analysis tool and is used to ensure that the plant operates in safe and secure manner.

4.6.1. ELECTRICAL MODELING OF PROCESS UNITS

To develop a network topology for the Hydrogen-based steel plant, it is important to understand the steady-state characteristics of each unit. In general, most of the units in the steel process are driven by motors. Therefore, it is important to select motors that are easier to control for the steel plant. Within the plant, most of the loads within the plant are modeled as synchronous motors because it can adjust to fluctuating load con-

ditions and has accurate speed control [45]. Which makes them suitable for mill applications and processing lines that require precise sizes to ensure high-quality products. The Electric Arc Furnace and Ladle Furnace are lumped as low voltage loads supplied by dedicated furnace transformers.A mill will at least have one stand, and each stand can be driven by one or two motors [46]. In this study, the Slab Caster, Hot Strip Mill, Skin Pass Mill, Cold Mill, and Finishing Mills are modeled as synchronous motors, along with processing lines such as the Annealing Line and Pickle Line [47]. The DR Shaft's primary energy consumption is met by burning fossil fuels [48]. Its electrical consumption consists of air blowers and compressors. However, in a Hydrogen based-route, electric heating substitutes the thermal reaction that usually supplies heat [49]. Unit 13, the Electric Heater is placed in the energy model to supply heating for the DR Shaft. The Electric Heater is modeled as a resistive load and the DR Shaft is a lumped induction motor. Note that the power factor of the PEM and Electric Heater is equal to 1 to because they are DC loads.

Table 4.8 contains the load list for all process units in the steel plant. The Load Type presents how each unit is modeled electrically in the power flow analysis. IM and SM represent induction and synchronous motors, respectively. The Voltage Level is the node voltage that is connected for each load. The Peak Consumption of each unit is calculated up to two decimal places by assuming the upper bound in constraint **??** and the values in Table 4.1. For example, at an hourly timestep,the parameters for the EAF $c_i = 494kWh/tonne, \beta_i = 100tonne$ and $d_i = 24.7kWh$ has a peak consumption at 49.42 MW. Where applicable, load ratings are selected based on manufacturer datasheets that designed motors intended for each process unit. The first digit is the number of motors required to supply the process unit multiplied by the motors nominal rating in MW Note that the selected motor ratings are higher that than rated energy consumption for each motor-driven unit. The higher selection is justified by taking into account any losses in energy conversion process. DC loads such as the PEM and Electric Heater are rated according to the rectifier that supplies them.

4.6.2. ELECTRICAL MODELING IN PANDAPOWER

A review in the literature indicates that steel manufacturers tend to operate in a radial network [50], [56]. Which is also confirmed after discussions with a Power System Expert in DNV. Based on voltage levels and power ratings, an N-1 radial network is proposed for the time series power flow analysis in Figure 4.12. This topology is validated by assuming a load flow scenario where the plant is required to produce at least 750 tonnes of cold-rolled, 150 tonnes of Hot Band and 1 tonne of hydrogen by the end of the production schedule. The results of the Gurobi optimization model are used as input for the pandapower power-flow timeseries simulation. This includes the consumption data for the units, and the generation data for the solar,wind, battery and fuel cell. Reactive power is calculated by assuming the power factor values of each load from Table 4.8. Since each load is supplied by its own transformer, the rating of the transformer is sized by assuming a 10% increase from the peak consumption of load. In pandapower, solar,wind, fuel cell and the battery are modeled as static generators. Note that the charging and discharging of the battery is controlled externally in the optimization which is why its not modeled as a storage element. Furthermore, it is assumed that static generators operate at the rated

Table 4.8: Electrical Load Parameters for All Units

Unit	Load Type	Voltage Level (V)	Peak Consumption (MW)	Load Rating (MW)	Power Factor	Reference
Arc Furnace	AC	415	49.42	-	0.78	[50], [51]
Ladle Furnace	AC	415	3.00	-	0.80	[50]
Slab Caster	SM	3300	16.50	1 x 17.2	0.85	[52]
Hot Strip Mill	SM	3100	284.17	14 x 20.3	0.80	[52]
Skin Pass Mill	SM	3300	0.52	1 x 0.56	0.85	[53]
Pickle Line	SM	3300	25.33	1 x 25.8	0.85	[52]
Cold Mill	SM	3100	37.78	8 x 4.8	0.85	[52]
Annealing Line	SM	3300	23.33	1 x 25.8	0.85	[52]
Finishing Mill	SM	3100	20.11	1 x 20.3	0.85	[52]
DR Shaft	IM	3300	32.22	2 x 18	0.85	[52]
PEM	DC	6000-36000	283.85	-	1.00	[54]
Condenser	IM	3300	0.86	1 x 0.9	0.85	[53]
Electric Heater	DC	450 V (DC)	2.18	-	1.00	[55]

voltage of their respective connection buses, as defined by the radial network model.

Units with the same voltage levels are supplied from the same bus. Both main transformers (TX-1 and TX-2) should be able to supply the entire network when the other transformer is out of service. The network is supplied by an external grid that is modeled as an infinite bus. The rating of each main transformer is selected to be 300 MVA where the high voltage is rated 150 kV and the low voltage side is 33 kV[57].The transformer rating is selected after iterating multiple load flow scenarios, where one main transformer can supply the network without exceeding 80% of its loading. Except for the EAF and LF, the voltage drop across all transformers in the network is selected to be 10%. To capture the chaotic nature of the EAF and LF, it is selected to be 21% and 18% [51].

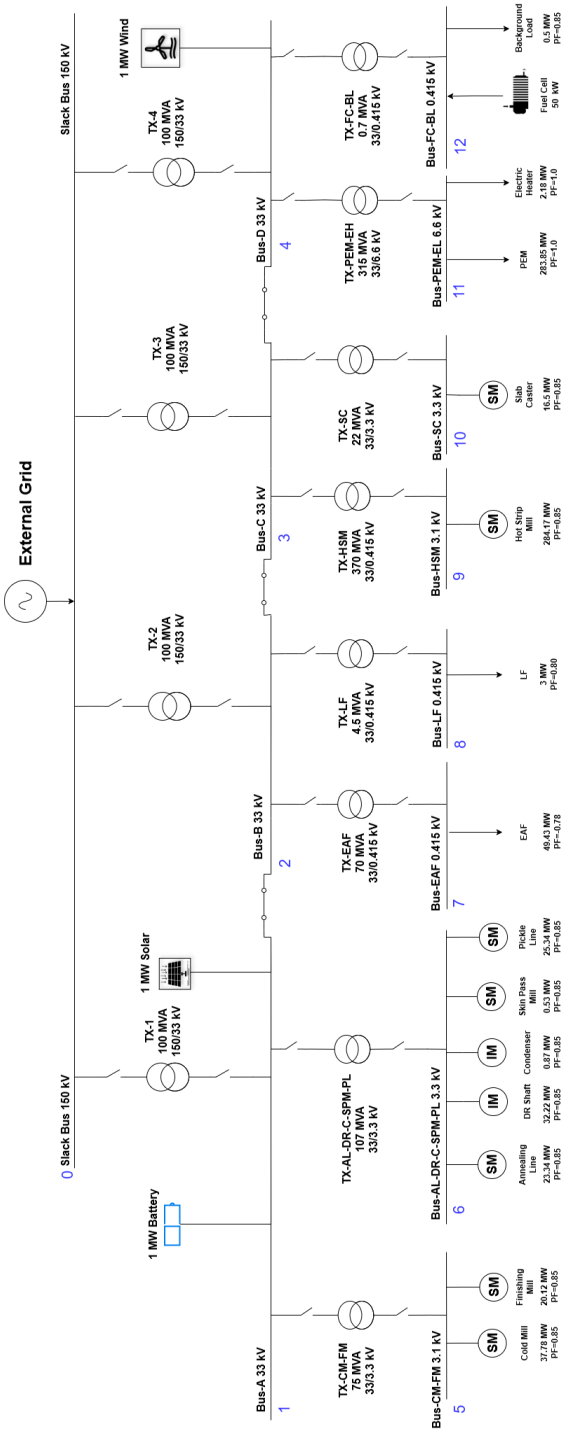

Figure 4.12: Proposed Radial Network Topology for a Hydrogen-Based Steel Plant

5

Chapter 5: Results and Discussion

5.1. MODEL VALIDATION AND FIXED PRICE SCENARIO

A steel manufacturer can secure a fixed electricity price by entering a bilateral agreement with a generator. This scenario is assumed to illustrate the behavior of such a manufacturer. Figure 5.1 shows the operational states of the Gantt chart for the units within the scheduling horizon. In this scenario, the plant operates with a rather sequential operation that aligns with the process design in Figure 4.5. Unit 11 (PEM) produces and stores hydrogen(k=23) until t = 14. Before any hydrogen is supplied to the DR Shaft,the Electric Heater heats up hydrogen and outputs heated hydrogen (k=24) in 1 batch cycle. Which then forces the operation of the DR shaft in the subsequent hour after the Electric Heater is switched on, because heated hydrogen cannot be stored. This behavior is depicted when materials that cannot be stored (k=8,9,24,25) are produced.It can be seen by observing the operational states of the units that produce such materials, which are the sequential operation for the combination of Units 1 and 2; 2 and 3 ; 10 and 12; and 13 and 10. Furthermore, the sequential operation between all of the units is validated by comparing it with the process design in figure 4.5. Each unit is operating when its input material is produced. Furthermore, the batch-cycle constraint is validated. When a unit is switched on, it has to operate for a minimum number of hours. For example, unit 8 (Annealing Line) has a batch cycle of a=6 hrs. At times t=32 and t=38, the unit switches on and remains on for 6 consecutive hours.

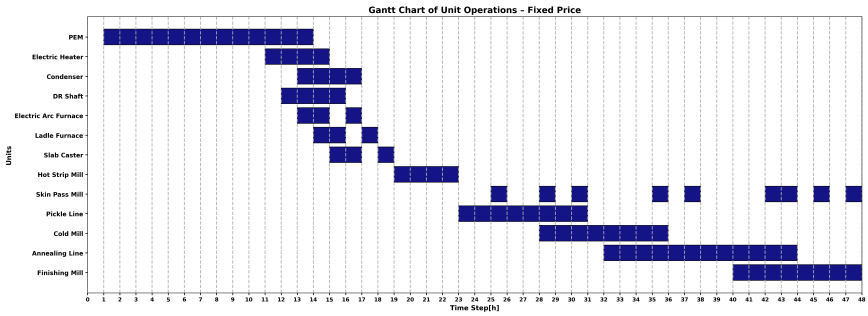

Figure 5.1: Production Schedule Under a Fixed Price Scenario.

The model is further validated by investigating the decision variables associated with each unit and material. Figure 5.2 shows the operational state,energy use , material flow and starting and ending times for the batch cycle of Unit 4 (Hot Strip Mill). There are two batch-cycle operation for this unit, at t= 18 and t=41 which aligns with the production schedule in figure 5.1.As mentioned in subsection 4.4.1, decision variables $s_i[t]$ and $e_i[t]$ are created to keep track of the batch cycle time. A unit will only start a batch cycle when $s_i[t]$-$s_i[t-1]$=1 , which can be observed at t =18 . Furthermore, it will respect the operational constraints in subsection 4.4.2 and remain ON ($x_i[t]$=1) according to its batch-cycle duration(a_4=4). The batch cycle will only end when $e_i[t]$-$e_i[t-1]$=1 which is observed at t=22. When the batch cycle begins, the unit will accept material according to the defined minimum (α_4=100 tonne) and maximum (β_4=100 tonne) capacities enforced by the constraints in subsection 4.4.4. When the batch cycle ends (t=22), the

same amount of material that entered the unit leaves the unit based on the capacity boundaries defined for the unit. When material is present inside the unit, it is processed to create new materials, which consumes electrical energy according to the constraints defined in 4.4.8.

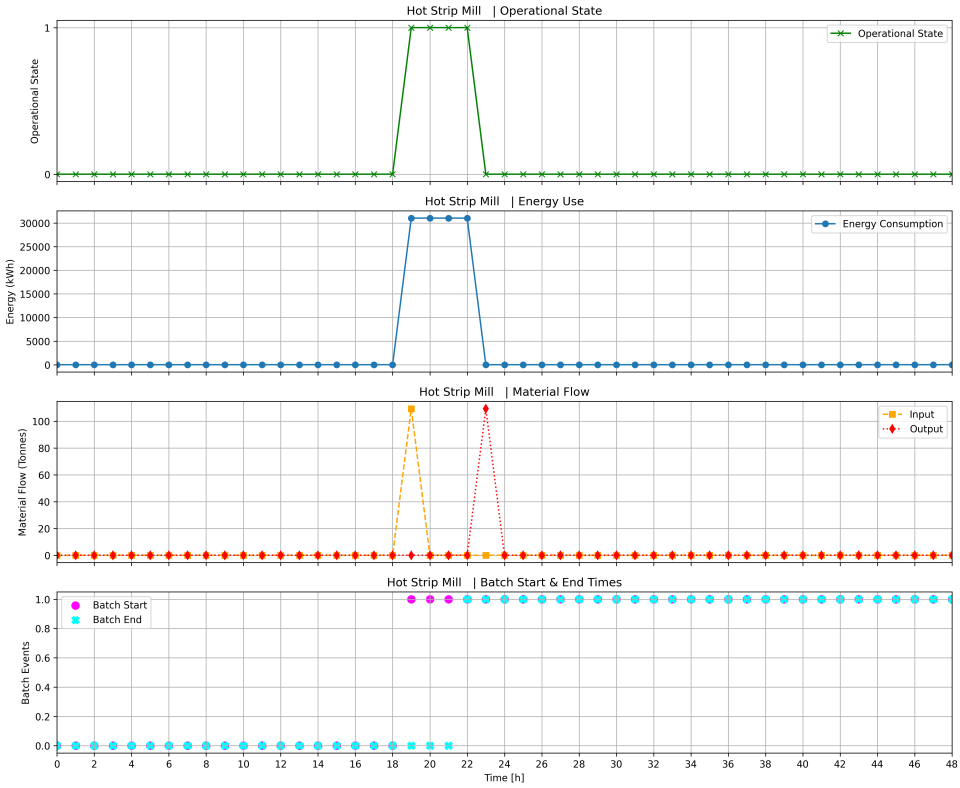

Figure 5.2: Operational States, Energy Consumption, Material Input and Output, Starting and Ending Batch Cycles for Unit 4(Hot Strip Mill)

Unit 9 (Finishing Mill) has a batch-cycle of 4 hours and a minimum and maximum capacities of 40 and 400 tonnes. Its operational state, energy use, material flow and starting and ending time for the batch cycle is in figure 5.3. This unit accepts Annealed Band (k=16) and produces Home Scrap (k=1), and Cold Rolled (F) (k=17).When interacting with Unit 9, the proportionality value for Annealed band is $r_9^{11} = 1$, $q_9^1 = 0.05$ for Home Scrap, and $q_9^{17} = 0.95$ for Cold Rolled. figure 5.3 is the operational state, energy consumption , starting and ending time for the batch cycles for Unit 9. Whereas, figures 5.4, 5.5 and 5.6 track the storage profile for Home Scrap, Annealed band, and Cold Rolled (F) throughout the production schedule.At t=40, 360 tonnes of Annealed band are taken from storage and loaded into Unit 9 and is processed until t=44. As a result, 342 tonnes of Cold Rolled (F) are produced (i.e. 0.95 x 360 tonnes). To ensure the material balance and proportionality constraints in 4.4.5, the remaining 18 tonnes must be produced as

Home Scrap (i.e. 0.05 x 360 tonnes) and this is supported by the increase Home Scrap storage from 10019,75 to tonnes 10038,08 Note that at t=44,Unit 9 accepts 380 tonnes of Annealed band because it is produced and supplied directly without storing the material.

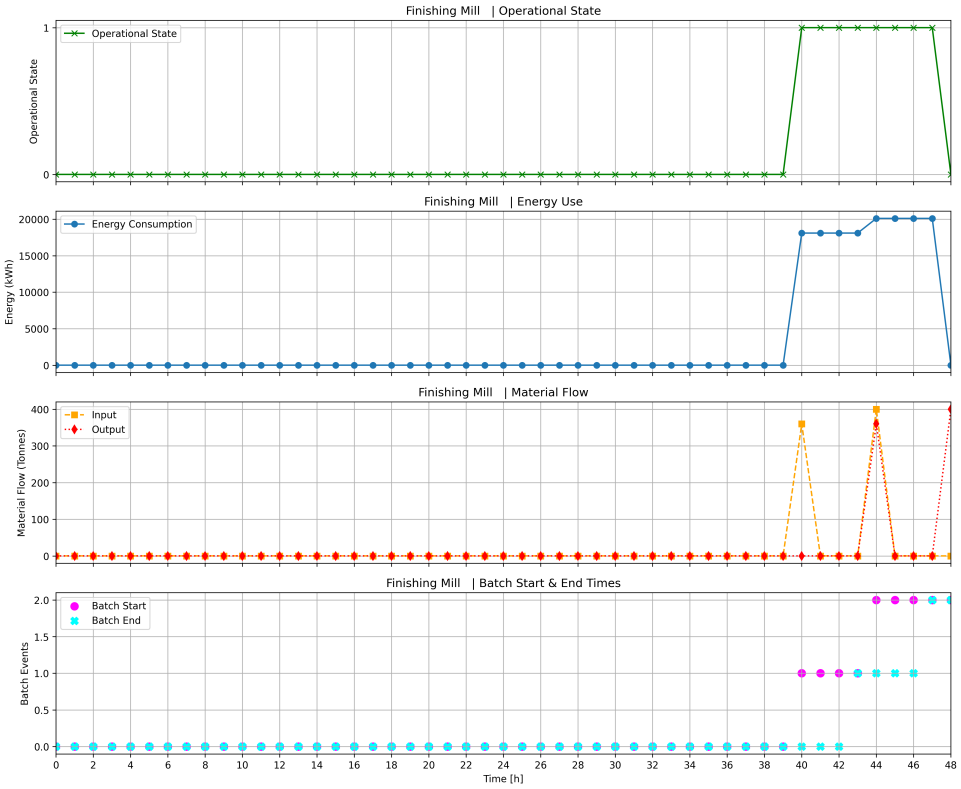

Figure 5.3: Operational States, Energy Consumption, Material Input and Output, Starting and Ending Batch Cycles for Unit 9(Finishing Mill)

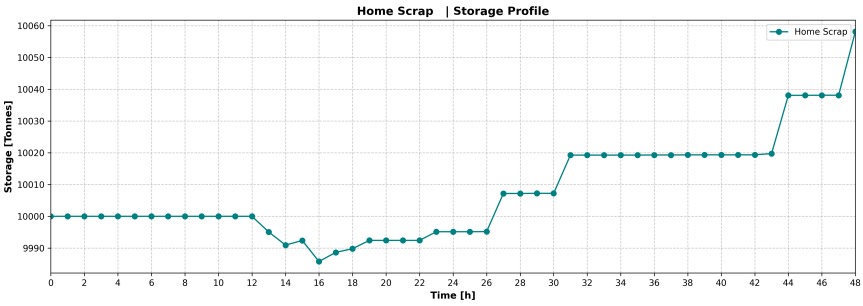

Figure 5.4: Material storage profile for home scrap.

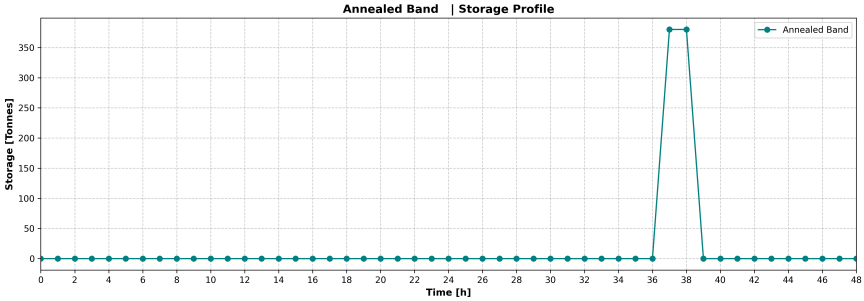

Figure 5.5: Material storage profile for annealed band.

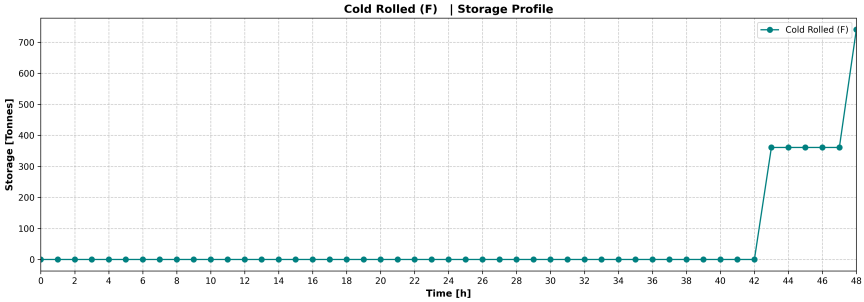

Figure 5.6: Material storage profile for cold rolled (F).

In the Fixed Price scenario, the steel plant generates a profit of € 211.078,43 by producing 722 tonnes of Cold Rolled (F) and 100 tonnes of Hot Band (F) throughout the production horizon. The carbon emissions are 0.0245 tonnes and the model is solved in 444,09s.

The total electrical energy consumption of the steel plant is shown in Figure 5.7. The plant depicts an energy profile that remains close to 150 MWh in the initial hours, which is associated with the operation of Unit 1 (PEM), the a highly energy intensive unit operating at full load approximately around 145.9 MW while the rest of the units are on standby consumption. At t=11, while the PEM is still operating at full load the Electric Heater operates and consumes 275 kWh of electrical energy. At t=13, the small energy rise is due to the DR Shaft consuming close 10 MWh of electricity. Peak consumption is at t= 14 when the PEM, Condenser, Electric Heater, DR Shaft and the EAF are operating and consuming close to 200 MWh of electricity. The rest of the plant's electricity consumption is dictated by the material loading of each unit and its batch cycle duration, which can be traced by linking the operational operational schedule of each from figure 5.1.

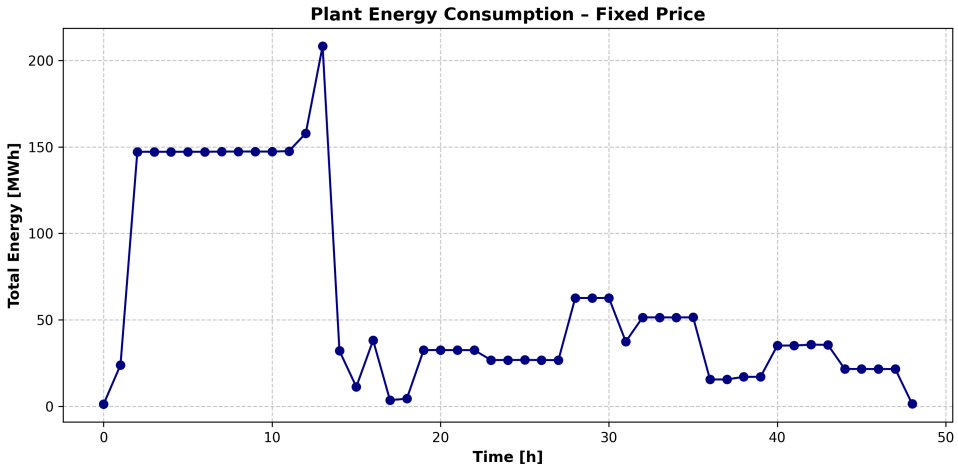

Figure 5.7: Total Energy Consumption of the HD-R Steel Plant

5

5.2. LOW PRICE SCENARIO

Figure 5.8 is the production schedule for the steel plant when exposed to low prices. When exposed to such a price profile, the steel plant produces 722 tonnes of Cold Rolled and 100 tonnes of Hot Band steel. The plant achieves a profit of € 262 185,20 with 0.0235 of CO_2 emissions. The initial operational of the units remain the same compared to the fixed price scenario, but in the low price duration from t = 22 to t = 29, the Skin Pass Mill operates at full load (40 tonnes) for two batch cycles and half load for one batch cycle at t = 25,26 and 27. In the fixed price scenario, it operates 9 batch cycles with varying capacities consisting of mostly the minimum capacity at 4 tonnes. Low prices shift the operating hour of the Skin Pass Mill under low price hours to meet the production requirement. Not only does the model demonstrate operational shifts, material loading is maximized at a low prices to maximize profit.

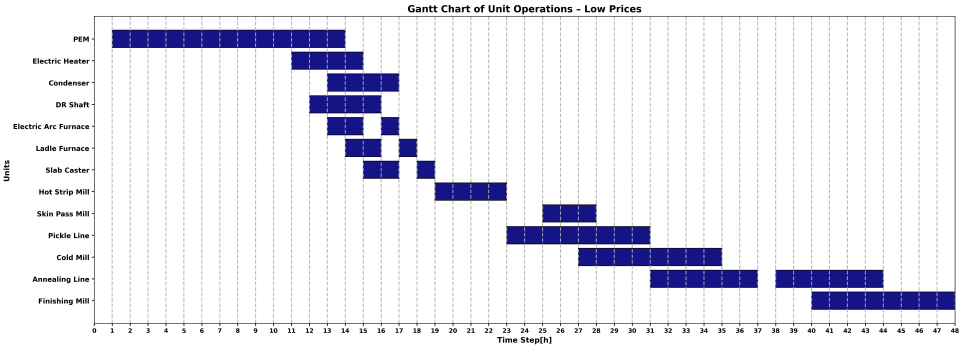

Figure 5.8: Production Schedule Under a low Price Scenario

The total energy consumption profile for the low price scenario is also shown in Fig-

ure 5.9. Compared to the fixed price scenario, there is a noticeable jump in electricity consumption at t =27 from 26.6 MWh to 62.7 MWh. Units 5,6 and 7 take advantage of the low price timeslot and operate compared to only unit 5 operating in the base case. The behavior of the model does not maximize production at low price periods. It opts to deliver on an optimal schedule with the focus on meeting production goal set in the production horizon.

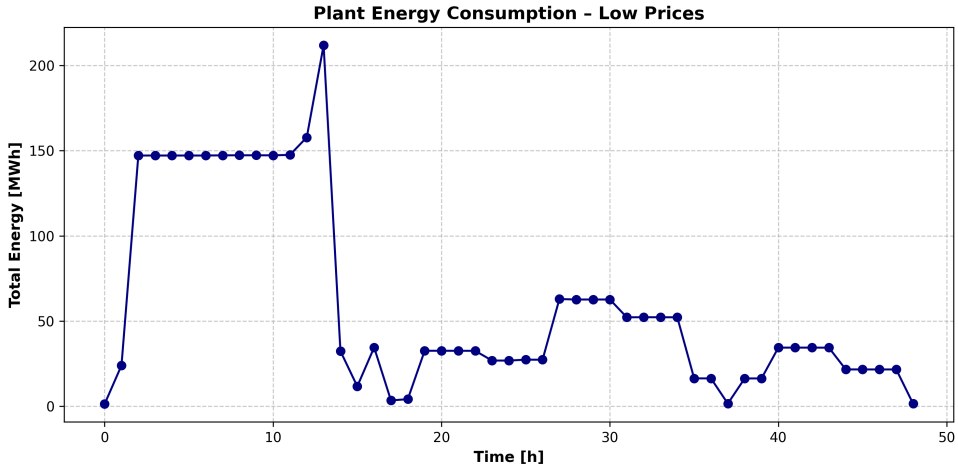

Figure 5.9: Total Energy Consumption of the HD-R Steel Plant Under a Negative Price Scenario

5.3. PEAK PRICE SCENARIO

The production schedule under a peak price scenario is in figure 5.10. In this scenario, the steel plant generates a profit of € 181,097.27 over the production horizon with Cold Rolled and Hot Band amounting to 722 and 100 tonnes, respectfully. This price profile introduces peak prices at t=18 and 19 for prices close to 0.45€/kWh. When compared to the fixed and low price scenarios,the Hot Strip Mill Does not schedule a batch cycle at t=19. Avoiding the peak price at t=19 and delays it till t= 20 where the price is approximately 0.22 €/kWh. Furthermore, the Cold Mill delays its second batch cycle to t = 34 where the cost of electricity is 0.1 €/kWh compared to the higher prices of 0.22 €/kWh and 0.26 €/kWh at t= 32 and t=33, respectfully.The Skin Pass Mill operates similarly to the low price scenario by operating two full and one half batch cycles. The only difference is the starting in the peak price scenario where the unit operates at the lowest price timeslot. Demand response demonstrates how the production schedule can work its way around a peak price without compromising production quota and attaining a profitable outcome.

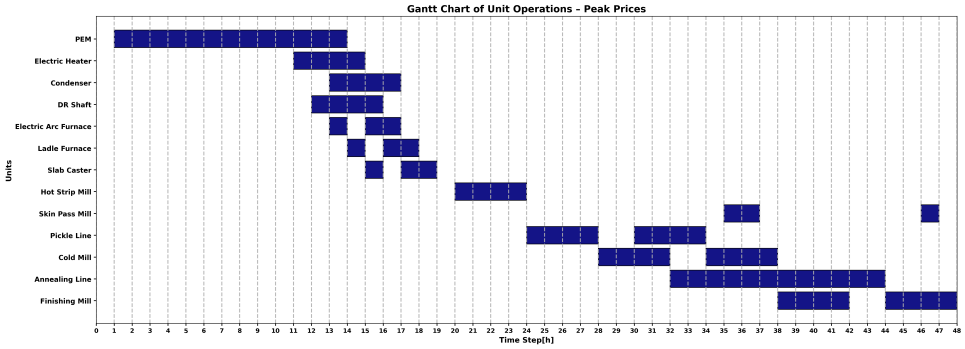

Figure 5.10: Production Schedule Under a Peak Price Scenario

The Energy consumption profile for this scenario can be seen in Figure 5.11. At t=16, the PEM schedules lower energy consumption for a price approximately at 0.18 €/kWh. This is highest price encountered by the PEM during its operational hours for this price profile. In addition, the plants energy consumption reduces to standby mode for the peak prices hours, where all units switched to standby mode at t=19.

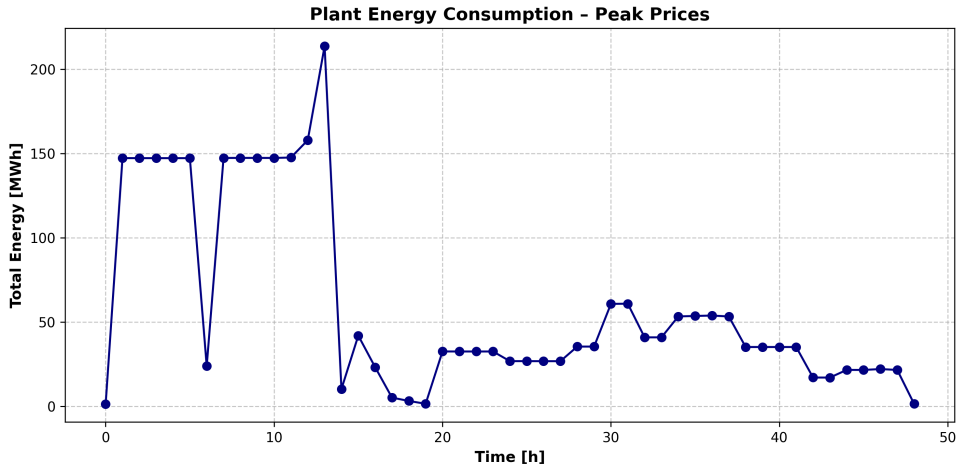

Figure 5.11: Total Energy Consumption of the HD-R Steel Plant Under a Peak Price Scenario

5.4. AVERAGE PRICE SCENARIO

Figure 5.12 presents the production schedule of the steel plant responding to the defined average price profile. In this scenario, the steel plant suffers from losses close to €97,795.70 to deliver 722 and 100 tonnes of Cold Rolled and Hot Band steel. The price profile has an average price of 0.2 €/kWh, where the higher price period coincides with the initial PEM operational hours. The plant takes a reserved approach to delivering the production requirement to minimize the losses encountered by the price profile.

Compared to the fixed price scenario, there is a shift in the starting time of the batch cycle for units such as the Skin Pass Mill, Cold Mill, Annealing Line, and the Finishing Mill. Furthermore, the EAF switches its second batch cycle from t=13 to t=14, which forces the LF and Slab Caster to also adjust their second batch cycle. There is a noticeable change in the batch cycle and material loading for the Skin Pass Mill. Originally, the unit had 9 batch cycles with full capacity at t=40, 33 tonnes at t=43, and the rest operating at a minimum capacity of 4 tonnes. In response to this price profile, it reduces the number of batch cycles to 3, operating at t=25, t=26, and t=47, when the prices are lowest in the profile (approx. 0.14 €/kWh).

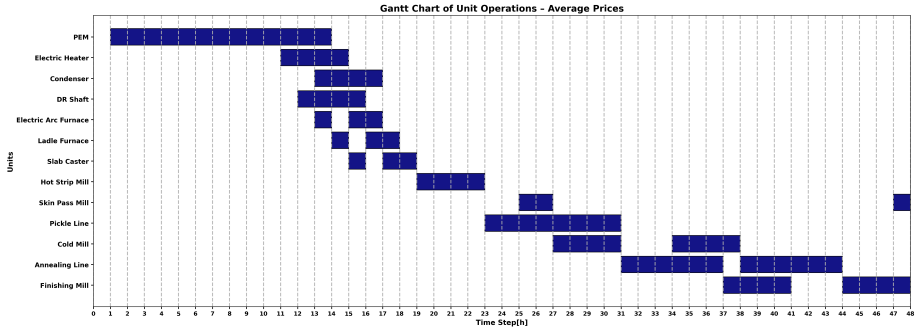

Figure 5.12: Production Schedule Under an Average Price Scenario

The energy consumption profile for this scenario is shown in Figure 5.13. There is a sharp decrease in energy consumption at t=8, associated with PEM reducing hydrogen production by 0.5 tonnes due to the highest electricity price of 0.27 €/kWh. In most scenarios, at least 33 tonnes of hydrogen are produced to meet the production quota at the end of the scheduling horizon.

The hydrogen reduction at t=8 is compensated by operating at full capacity at t=13, which justifies the peak consumption of 213 MWh at this hour. At this point, the PEM, DR Shaft, Condenser, Electric Heater, and EAF are operating. Beyond t=13, the plant resumes responsive operation by varying the starting time and material loading of batch units, shaping the overall energy consumption profile.

5.5. FUEL CELL

Figure 5.14 shows the energy and hydrogen consumption of the fuel cell in the low price scenario, which is the exact fuel cell profile for the rest of the pricing scenarios.It can be seen that when 2.5 kg of H_2 is supplied to the fuel cell, and the fuel reaches its rated electricity production at 50 kWh. Under all price scenarios, the fuel cell will switch on after the PEM produces enough hydrogen to meet the production requirement by the end of the schedule horizon.

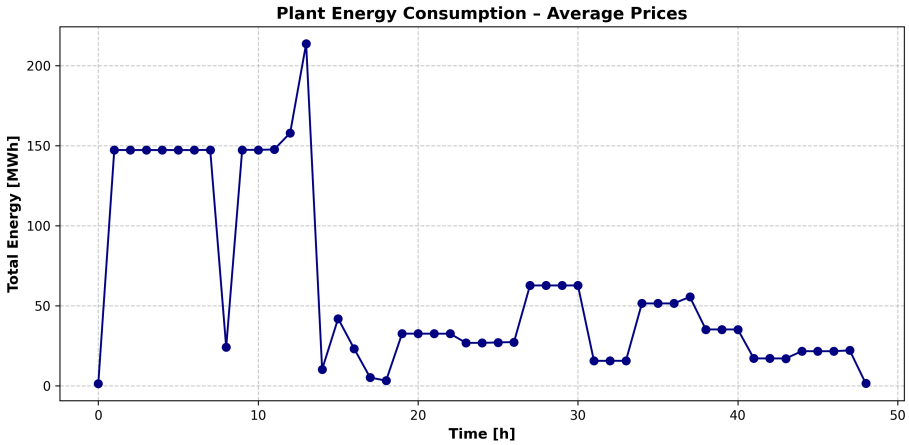

Figure 5.13: Total Energy Consumption of the HD-R Steel Plant Under an Average Price Scenario

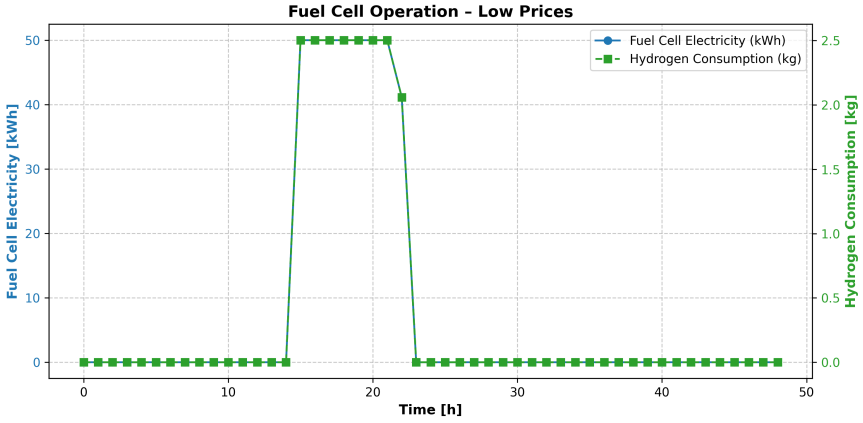

Figure 5.14: Fuel Cell: Electricity Generation and Hydrogen Consumption in Low Price Scenario

5.6. BATTERY

Figure 5.15, 5.17 and 5.16 show the battery capacity throughout the production schedule for the average, peak and low price scenarios.In the average price scenario, the battery is frequently charging and discharging in response to the constant high electricity prices. Consistent exposure to such a profile can decrease the state-of-health of the battery since its cyclic between full and zero capacities. In the peak price scenario, the battery remains charged before it encounters the peak price at t=18, and begins to discharge at the same instant to reduce the import of electricity from the network. In the low price scenario, the battery starts charging from t=24 to full capacity at t= 27 and remains full charged until t =32, surpassing the low price period and discharging momentarily at t=33. The charging and discharging times of the battery respond to electricity prices. For each price profile, the battery demonstrates a different behavior in response to the electricity prices. Which illustrates energy management without deploying advanced algorithms specific to the battery.

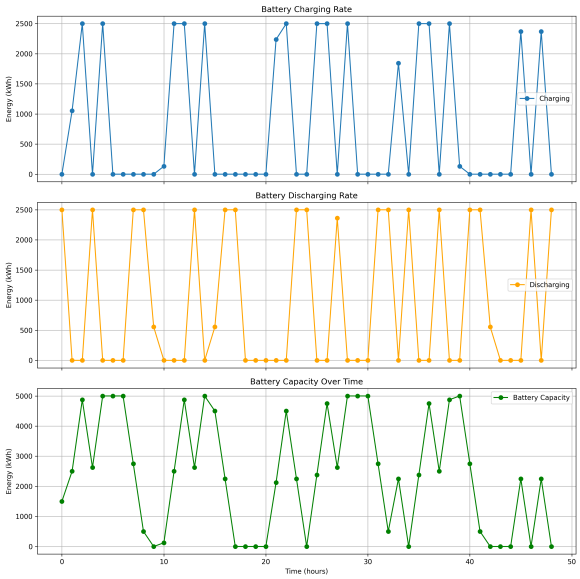

Figure 5.15: Average Prices: Battery Charging Rate (Top), Battery Discharging Rate (Middle), and Battery Capacity Over Time (Bottom)

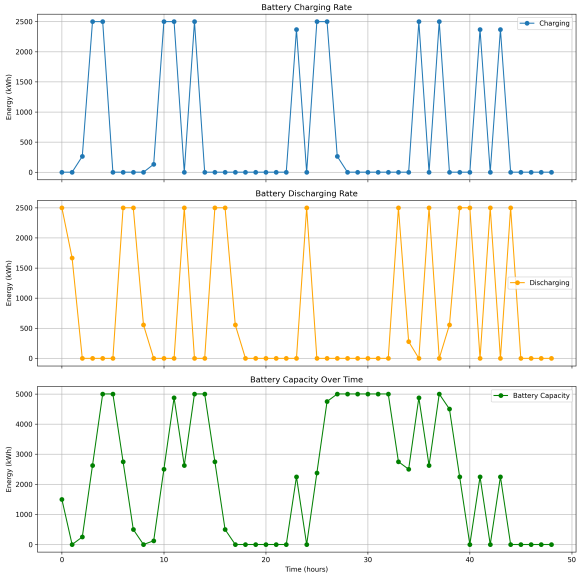

Figure 5.16: Low Prices: Battery Charging Rate (Top), Battery Discharging Rate (Middle), and Battery Capacity Over Time (Bottom)

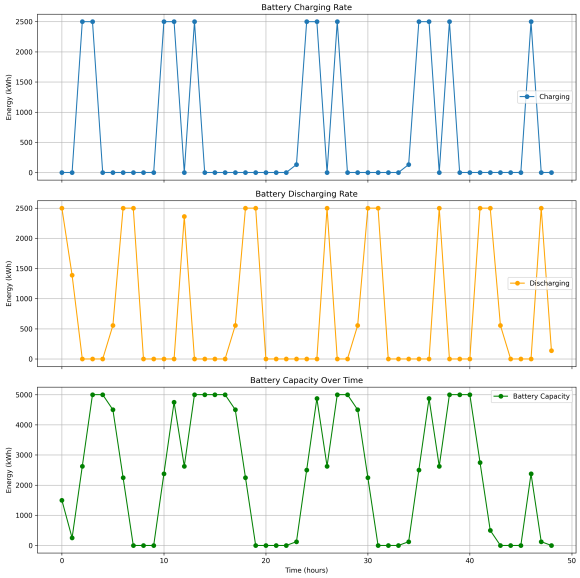

Figure 5.17: Peak Prices: Battery Charging Rate (Top), Battery Discharging Rate (Middle), and Battery Capacity Over Time (Bottom)

5.7. OXYGEN AND EAF ENERGY EFFICIENCY

Figure 5.18 is the amount of oxygen in storage and when is it supplied to the EAF. It should be noted that from t=3 till t=13 , the PEM is operating and also produces oxygen as a by product. At t=14, 29.05 tonnes of Oxygen is supplied to reduce the energy consumption of the EAF by 7179 kWh. Note that oxygen assimilates in storage up to 26.9 tonnes and the rest of the oxygen intake is supplied directly from the PEM at t=14.

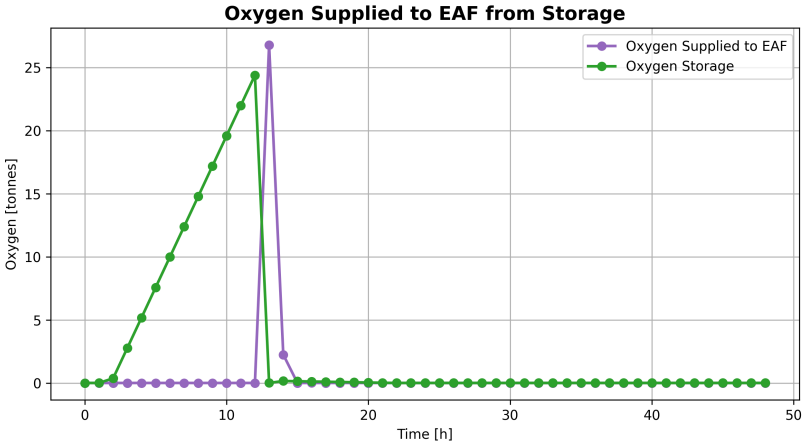

Figure 5.18: Oxygen Storage and Oxygen supplied to the EAF

5.8. SENSITIVITY ANALYSIS

5.8.1. INITIAL AMOUNT OF HYDROGEN IN AN AVERAGE PRICE SCENARIO

In the average price scenario, its insightful to understand what is the least amount of Hydrogen required such that the plant abstains from losses. Therefore, sensitivity analysis is carried out at the initial amount of Hydrogen during the production schedule while maintaining the original production quotas. Starting from 100kg of H_2 and increasing in steps of 100kg to uncover how much hydrogen is required to mitigate the losses of the plant. The results of the analysis are in figure 5.19.To avoid incurring any losses for this price profile, at least 700.8 kg of H_2 should be available at the beginning of the production schedule.If the steel plant has access price predictions, such analysis can reveal the how much H_2 should be in storage to avoid losses. It is also important to note that storage of H_2 is not the only way to address such a scenario.Purchasing DRI or replacing its proportionality input in the EAF with scrap steel can remove the need the initial amount of H_2 [15].

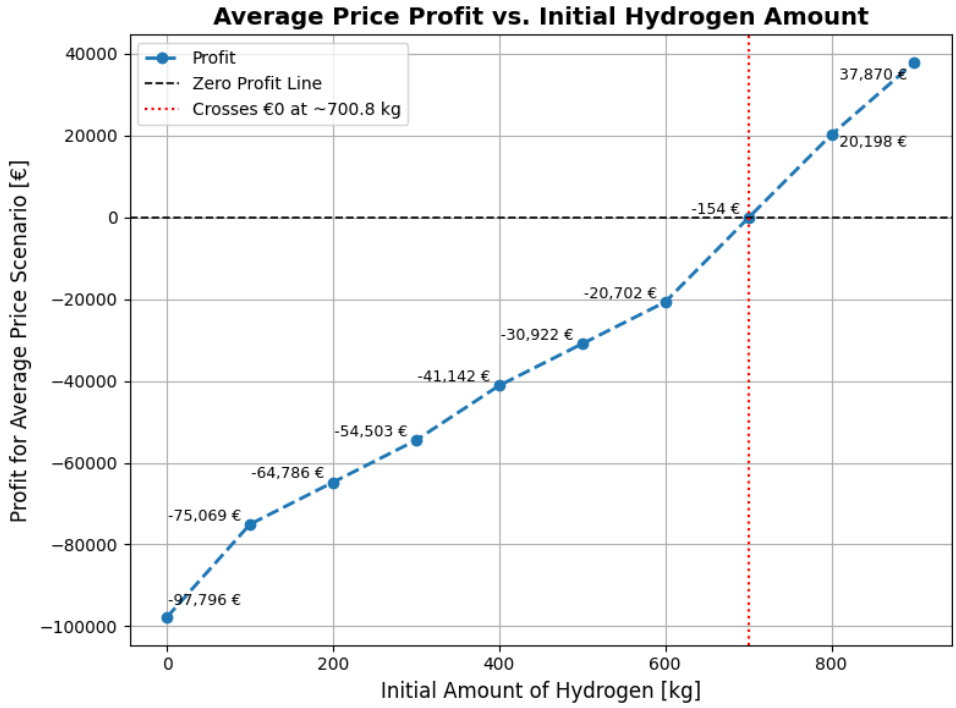

Figure 5.19: Average Price Scenario: Initial Amount of Hydrogen Sensitivity Analysis

5.8.2. FUEL CELL OPERATION AT LOW PRICES

Adding a fuel cell to the energy system requires further analysis. At low prices, when hydrogen is produced cheaply, sensitivity analysis is conducted in the fuel cell by varying its efficiency and rated power. The combination of varying both variables. First, the

Table 5.1: Impact of Fuel Cell Configuration on Profit, Energy Output, and Hydrogen Use under Low Prices

Fuel Cell: Rating and Efficiency (η)	Profit [€]	Operating Hours	Total Energy Produced [kWh]	Total Hydrogen Supplied [kg]
η = 0.6, Rating = 100 kWh	€262,364.60	4	391.16	0.02
η = 0.6, Rating = 150 kWh	€262,409.85	3	391.16	19.58
η = 0.6, Rating = 200 kWh	€262,409.85	3	391.16	19.58
η = 0.7, Rating = 200 kWh	€262,416.27	3	456.35	19.58
η = 0.8, Rating = 200 kWh	€262,422.70	3	521.54	19.58
η = 0.9, Rating = 200 kWh	€262,426.90	3	586.74	19.58
η = 0.9, Rating = 250 kWh	€262,429.10	3	651.93	19.58
η = 1.0, Rating = 250 kWh	€262,435.50	3	651.93	19.58

rating of the fuel cell is increased in steps of 50 kWh maintain the original 60% efficiency. There is no restriction on the hydrogen flow for the fuel cell. The results of the sensitivity analysis are in Table 5.1. Increasing the rating of the fuel cell reduces the operating hours of the fuel cell up to three hours only while the total volume of energy produced by the fuel cell remains the same. Efficiency is varied in steps of 10% to investigate its impact. This increases the total volume of energy until 586 kWh for a 200 kWh fuel cell with 90% efficiency. Beyond this point, the rating is increased to 250 kWh which increases the total volume energy produced to 651,9 kWh. Furthermore, even when assuming the a 100% efficiency fuel cell with no restriction on the hydrogen consumption, the fuel cell sees that it should only operate for three hours producing 651,9 kWh of electricity. For all the sensitivity analysis cases, the production quota remains the same at 722 and 100 tonnes for Cold Rolled and Hot Band steel.Note that increasing the efficiency and energy rating has a minor increase in profit compared to the low price scenario. Without considering operating and maintenance costs for the fuel cell, it may be useful to omit the fuel cell for the steel plant. Under favorable low price conditions, sensitivity analysis reveals that even when using a 100% efficiency fuel cell rated at 250 kW, without restricting hydrogen intake, increases the profit of the steel plant by only €250,3 when compared to a 50 kW fuel cell with 50% efficiency.

5.8.3. FLEXIBILITY UNDER PEAK PRICES

Flexibility is investigated under a peak price scenario to sell electricity when prices are high. While investigating the flexibility, the production quota is unbounded at first and then sensitivity analysis is carried out. It takes place by varying the value of ϵ from 0.0 to 1.0 in steps of 0.1, the total energy offered to the wholesale market can be seen at Figure 5.20. It can be noted, for each value of ϵ, the plant offers its energy at t=18 for a peak price around 0.45€/kWh, by selling electricity at the highest price. This contribution is associated with the PEM offering its almost 140 MWh of electricity, which is translated to €63,000 of profit for ϵ = 1.0. The

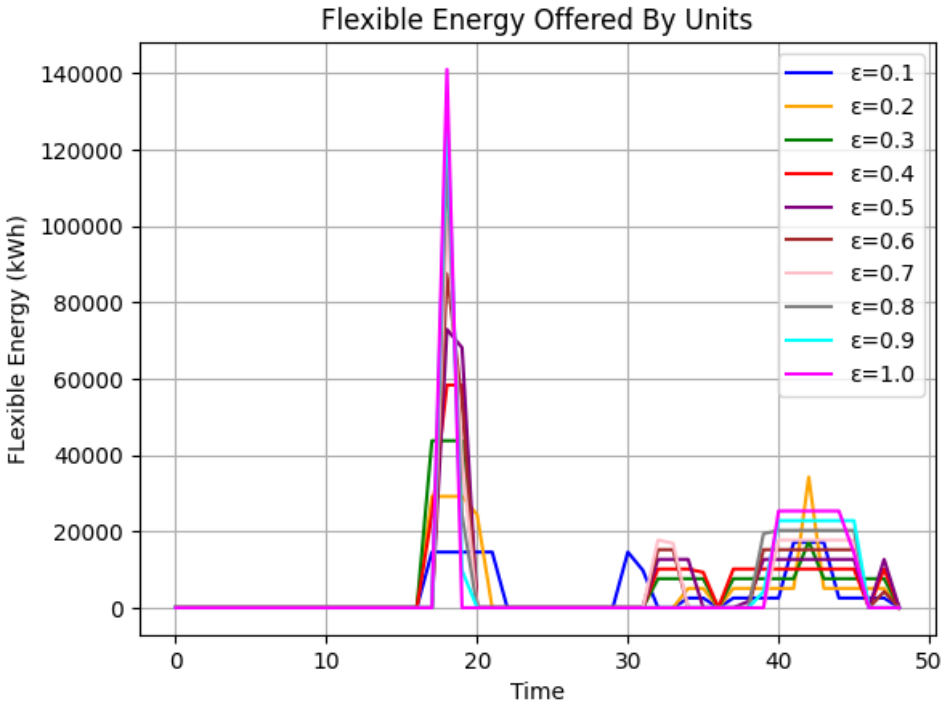

Figure 5.20: Sensitivity Analysis of ϵ Value to demonstrate energy offered by flexible units

Table 5.2 summarized the results of the sensitivity analysis for ϵ. The base scenario for this case is for $\epsilon = 0.0$. When unbounded by production requirements, the model opts to produce 722 and 90,79 tonnes of Cold Rolled and Hot Band steel, respectfully. Which generates a profit of € 213.819,24 in this scenario. Increasing the value of ϵ reduces the amount of Hot Band steel.When given the freedom, the model sees it more profitable to reduce Hot Band steel and favoring the offering its capacity to the wholesale market. The most notable increase in profit is when $\epsilon = 0.1$ achieving a profit of€ 231,859.70. At this value, the plant reduces it energy volume by 70.35 kWh and adjusts its energy profile compared to the peak base scenario. While incrementing the value of ϵ, the profit increases at a much lower rate compared to $\epsilon = 0.1$. This rate keeps on decreasing with more energy offered to the market until $\epsilon = 0.4$. Beyond this point, Hot Band output remains at 67.95 tonnes, while the profit increases by small margins.The small increases in profit suggests that the plant can trade electricity in by redistributing the same volume of energy of the flexible units more efficiently. At $\epsilon = 1.0$, the profit margin compared to the base peak scenario is close to €76,000, with €63,000 generated by the PEM, and the rest of the flexible units contribute accordingly. The increase in profit when ϵ increases is not only justified by the offered flexibility and volume of energy reduced, there is a noticeable shift in the plants energy consumption for $\epsilon = 0.5$ and $\epsilon = 0$ as seen in figure 5.21. The shift is a result of the steel plant selling electricity and adjusting the profile to meet production requirements by the end of the schedule.

Table 5.2: Flexibility impact on plant performance under peak prices.

ε	**Hot Band [tonnes]**	**Profit [€]**	**Energy Reduction Compared to Peak Scenario [kWh]**
0.0 (Peak Scenario)	90.79	€ 194,171.20	0
0.1	85.46	€ 231,859.70	70.35
0.2	80.12	€ 244,134.95	140.70
0.3	72.33	€ 252,203.70	243.80
0.4	67.95	€ 259,208.10	301.48
0.5	67.95	€ 265,142.66	301.48
0.6	67.95	€ 266,489.72	301.48
0.7	67.95	€ 267,714.87	301.48
0.8	67.95	€ 268,874.40	301.48
0.9	67.95	€ 270,047.30	301.48
1.0	67.95	€ 271,072.65	301.48

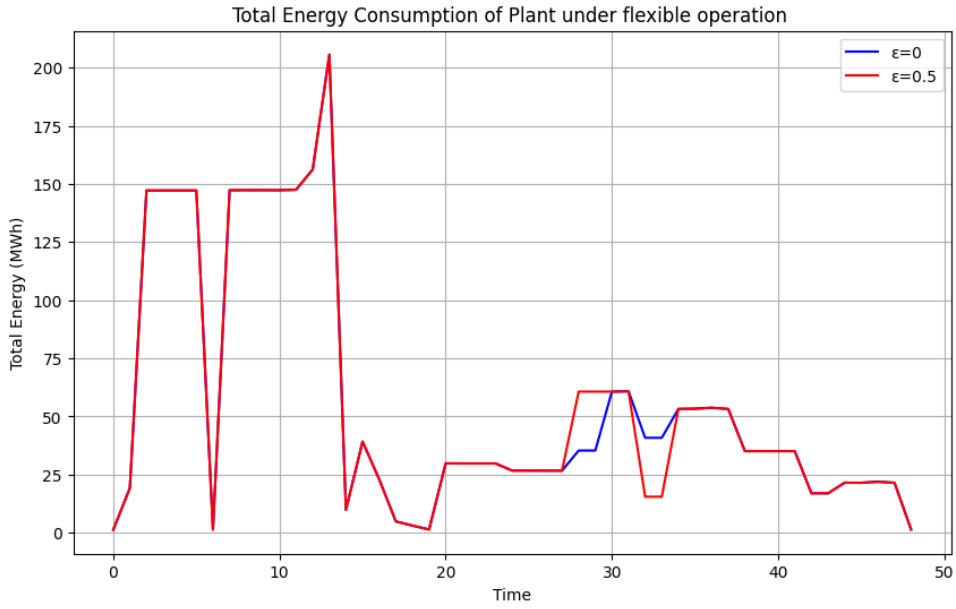

Figure 5.21: Total Energy Consumption of Plant under flexible operation

5.9. TIMESERIES POWERFLOW

To assess the electrical performance and reliability of the plant network, a time-series power flow analysis is conducted under different transformer operating scenarios. The

primary focus is on evaluating transformer loading, voltage levels at critical buses, and identifying violations of operational limits. Three operating conditions are considered,Normal operation with all transformers in service,TX-1 out of service and TX-1 and TX-2 out of service.These scenarios reflect common maintenance or contingency situations. The results are used to validate the robustness of the network, explain transformer loading behavior, and justify voltage fluctuations caused by key industrial units such as the Electric Arc Furnace (EAF) and Ladle Furnace (LF).

5.9.1. NORMAL OPERATION WITH ALL TRANSFORMERS IN SERVICE

Suppose a plant operation where all main transformers operate, the percentage of loading for each transformer is shown in Figure 5.22. It can be seen that all 4 transformers share their load capacity equally and none of the transformers exceeds 80% load capacity, which is the standard practice in industry. The slight variations in the transformer loadings are because of the network topology and production schedule. For example, TX-4 is slightly loaded than the other transformers from t = 0 to t = 12 and from t = 20 to t = 28, because these are the operating times of the PEM which is supplied by TX-4 from Bus-Coupler D. Figure 5.23 shows how the bus voltages vary throughout the production schedule for this operation mode. Most of the buses operate with acceptable limits except for Bus 33 kV B and the buses that supply the EAF, LF, and CM-FM. The EAF and LF violate the limits because of their low power factors(0.78 and 0.80) and higher transformer voltage drops(21% and 18%) for the voltage transformers. At t=29, the EAF has a bus voltage of 0.92, which causes Bus-33 B and its connected loads to violate its operational limits. Furthermore, the dip distorts the voltage stability of the other buses within the plant. Note that for all transformer scenarios, none of the downstream transformers exceeds 80% of its loading capacity.

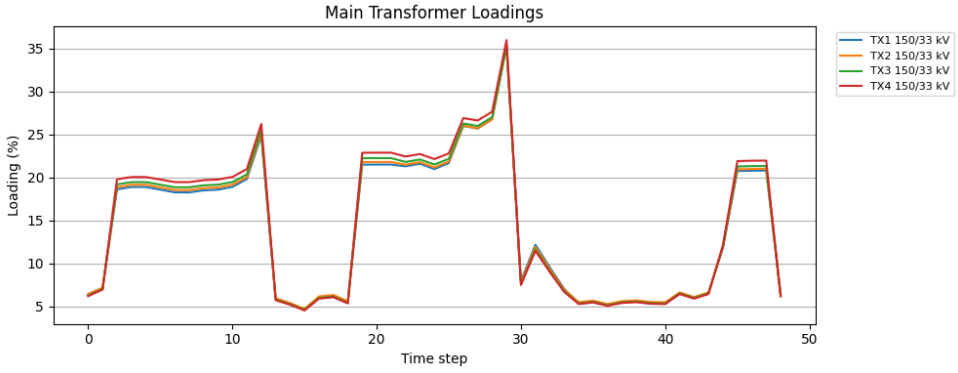

Figure 5.22: TX-1,TX-2,TX-3 and TX-4 Loading Under Normal Operation

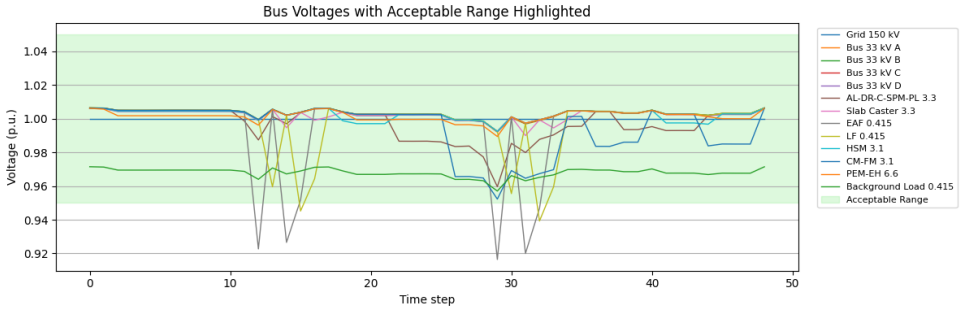

Figure 5.23: Bus Voltages Under Normal operation

5.9.2. TX-1 OUT OF SERVICE

Now, assume that TX-1 is out of service for maintenance for the same production schedule. Figure 5.24 shows the transformer

loading for TX-2,Tx-3, and Tx-4. They adapt to the plant load requirements by breaching 80% at t = 29, to provide peak consumption. In general, loading a transformer above 80% is permissible but not recommended. In this scenario, bus voltages follow the same trend as normal operation, with the exception of Bus AL-DR-C-SPM-PL 3.3, which also breached the limits at t=29.

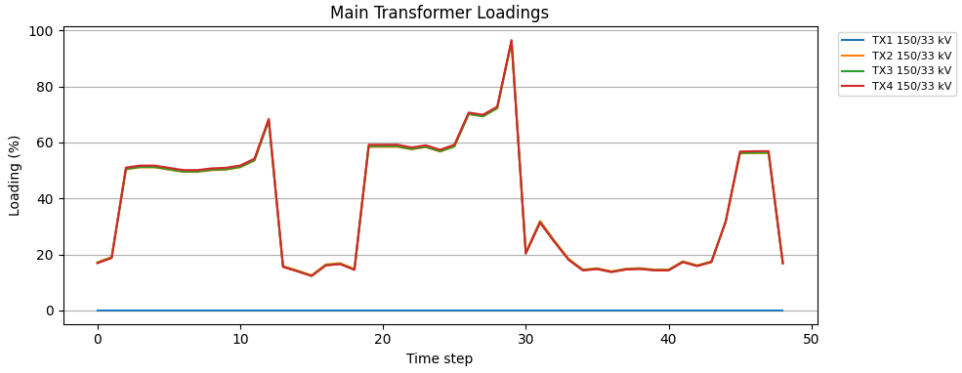

Figure 5.24: TX-1,TX-2,TX-3 and TX-4 Loading Under When Tx-1 is out of service

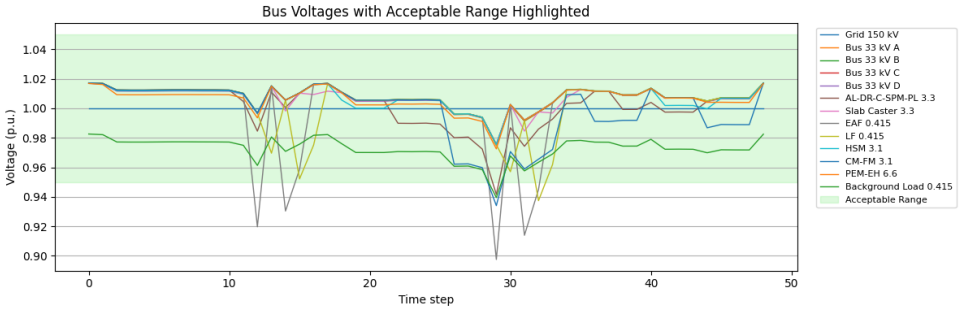

Figure 5.25: Bus Voltages When Tx-1 is out of Service

5.9.3. TX-1 AND TX-2 OUT OF SERVICE

Finally, assume that TX-1 and TX-2 are out of service for the same production schedule. As shown in Figure5.26, from t=26 to t=29, TX-3 and TX-4 are overloaded and reach a loading capacity up to 158.4% at t=29. Which is equivalent to an active and reactive power consumption of 139.5 MW and 75.2 MVAr, per transformer. Operating at a 0.88 lagging power factor, which is considered acceptable subject to the agreement with the grid connection provider.

Furthermore, as per IEEE Std C57.91 [58], transformers can be loaded up to 200%, which could be either planned or emergency operation. Since steel plants are usually private networks, the plant operator can plan overloading. However, this should be carried out after identifying the limitations of the power transformers, which comes with operator experience and identifying thermal spots in the transformers. Figure 5.27 shows the bus voltages when TX-1 and TX-2 are out of service. Similarly to only TX-1 out of service, the same buses that are within acceptable and unacceptable limits. Its observed that the EAF operates at 0.875 p.u at t=29, compared to 0.9 p.u.

Figure 5.26: TX-1,TX-2,TX-3 and TX-4 Loading When TX-1 and TX-2 are out of service

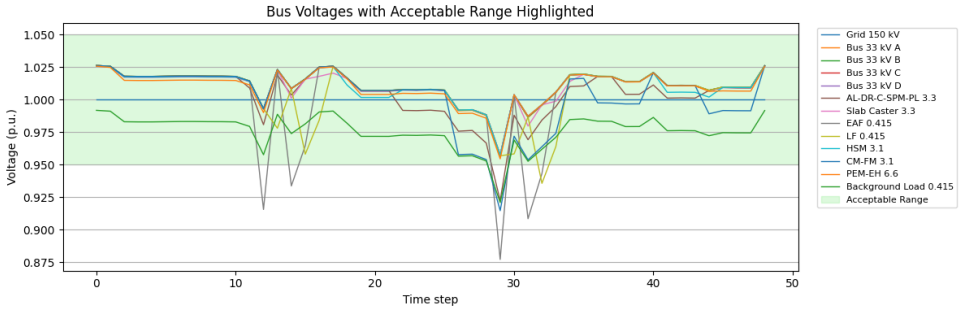

Figure 5.27: Bus Voltages When Tx-1 and TX-2 are out of Service

5.10. STEEL PLANT IMPACT ON HIGH VOLTAGE GRID

When independent plant operation is established and considered acceptable in the worst-case scenario, the peak active and reactive power consumption of the plant is modeled as a static load in the European High-Voltage Case89Pegase grid [59], [60]. The network only available in data format, has 89 buses, 12 generators, 210 branches that operate at 380,220 and 150 kV. The data used in this grid are not from an actual grid, but is actually created to capture the size and complexity of an actual high-voltage grid in Europe. There are 34 150 kV buses where 22 loads are connected. In its worst case scenario, the plant is consuming 278.5 MW and 150.9 MVAr, which is used to model a load connected to a vacant 150 kV bus. Note that the data is used in the case file is for a single instant, and the steel plant impact is considered for that moment. There are 13 150 kV vacant buses and the steel plant is separately connected to each bus as a scenario. Accordingly, power-flow analysis is conducted to see the impact of the plant on the line loadings and bus voltages. Table 5.3 shows the lines that exceed an 80% loading limit for at least one scenario, where the column headings are the buses where the steel plant is connected for each scenario. When compared to the base case, 6 lines are exceeding an 80% capacity without the steel plant connection. while Line 86(below 80% in base case) shows a 4% increase in loading to when the plant is connected to bus 1530, which may apply line upgrades depending on the TSO requirements. It should be noted that Line 94 is overloaded which can be acceptable for short durations and is usually well accounted for by operator experience.

Table 5.3: Line Loading (%) Across Different Bus Injection Scenarios

Line #	Line (From — To)		Base Case	Bus 227	Bus 1530	Bus 3278	Bus 3505	Bus 4013	Bus 4422	Bus 4585	Bus 5096	Bus 5586	Bus 7278	Bus 8228	Bus 8419
	From Bus	To Bus													
13	1967	8963	93.91	93.04	93.73	93.02	98.00	93.79	93.55	93.24	94.00	93.43	93.79	89.08	94.10
33	3492	5586	85.45	82.34	87.32	85.45	88.38	87.00	84.90	71.36	87.26	36.30	87.00	85.63	88.68
72	954	3505	85.34	85.73	85.37	85.66	58.69	85.21	85.16	85.40	84.96	85.26	85.21	90.71	84.60
86	791	3278	79.65	78.98	83.61	36.84	79.56	81.67	79.55	79.17	80.34	79.46	81.67	78.36	80.20
94	5415	7636	100.92	100.92	100.92	100.92	100.92	100.92	100.92	100.92	100.92	100.92	100.92	100.92	100.92
95	8963	2167	81.25	81.97	81.53	81.78	89.55	81.42	81.76	81.73	81.31	81.85	81.42	85.87	81.50
159	1610	8419	81.98	82.93	83.90	83.07	82.64	85.07	83.46	82.98	88.16	83.38	85.07	82.41	42.27

The impact of the steel plant on other bus voltages is in Table 5.4. These are the buses that operate outside of acceptable limits in at least one scenario.When the plant is connected to bus 1530, voltage magnitude decreases for the listed buses, where all of

the buses except 791 and 3278 operate outside of the acceptable limits. Furthermore, buses 954,6832 and 7179 undergo greater voltage drops which could damage the lines and reduce its lifespan. The voltage decrease can be mitigated by introducing capacitor banks that can supply reactive power by restoring the buses to acceptable limits.In reality, the grid impact of the plant will depend on its geographical location and the feeder availability from the TSO. These results are used to illustrate how geography can play a role by considering the peak consumption of the plant on an illustrative high voltage European grid.

Table 5.4: Voltage Magnitude (p.u.) for Selected Buses under Different Steel Plant Connection Scenarios

Bus	**Base**	Bus 227	Bus 1530	Bus 3278	Bus 3505	Bus 4013	Bus 4422	Bus 4585	Bus 5096	Bus 5586	Bus 7278	Bus 8228	Bus 8419
791	0.9853	0.9853	0.9789	0.9476	0.9850	0.9847	0.9849	0.9854	0.9851	0.9850	0.9847	0.9854	0.9850
954	0.9568	0.9559	0.9557	0.9566	0.8948	0.9564	0.9551	0.9565	0.9566	0.9551	0.9564	0.9509	0.9549
1967	0.9778	0.9766	0.9768	0.9778	0.9489	0.9774	0.9764	0.9775	0.9776	0.9763	0.9774	0.9678	0.9765
2167	0.9703	0.9692	0.9693	0.9703	0.9405	0.9699	0.9689	0.9700	0.9701	0.9688	0.9699	0.9614	0.9690
2267	0.9552	0.9542	0.9537	0.9547	0.9435	0.9546	0.9536	0.9546	0.9548	0.9536	0.9546	0.9521	0.9539
2440	0.9501	0.9494	0.9494	0.9499	0.9279	0.9499	0.9491	0.9498	0.9501	0.9491	0.9499	0.9459	0.9493
3278	0.9853	0.9854	0.9790	0.9475	0.9851	0.9848	0.9849	0.9854	0.9851	0.9850	0.9848	0.9854	0.9851
3505	0.9571	0.9562	0.9559	0.9569	0.8949	0.9567	0.9554	0.9568	0.9569	0.9553	0.9567	0.9512	0.9552
6068	0.9368	0.9359	0.9358	0.9365	0.9167	0.9364	0.9355	0.9364	0.9366	0.9355	0.9364	0.9310	0.9358
6292	0.9537	0.9530	0.9530	0.9534	0.9345	0.9534	0.9527	0.9533	0.9536	0.9527	0.9534	0.9496	0.9529
6832	0.9277	0.9267	0.9266	0.9274	0.9064	0.9273	0.9263	0.9272	0.9275	0.9263	0.9273	0.9214	0.9266
7179	0.9301	0.9291	0.9291	0.9298	0.9087	0.9297	0.9288	0.9297	0.9299	0.9287	0.9297	0.9238	0.9290
8963	0.9702	0.9691	0.9691	0.9701	0.9403	0.9698	0.9688	0.9699	0.9700	0.9687	0.9698	0.9612	0.9689

The results of all assumed scenarios, along with the codes and a summary of the results can be found in the Appendix.

6

Conclusion

An energy system for a hydrogen based steel plant is modeled using a smart industrial load for batch-based processes. The model is extended with energy efficiency factors such as oxygen supply to the EAF, DR Shaft warm up time, and flexible units that can offer energy capacity to the electricity market. The model depicts unit behavior according to its sequential relationship with other units, and the proportionality of the materials that enter and leave a unit. Energy consumption is based on the amount of material processed by a unit bounded by the minimum and maximum capacity of the unit. Starting and ending times are respected according to the batch cycle duration of each unit. Uninterruptibility of units is captured based on their process design. The model responds to electricity prices by adjusting the energy profile of the plant and varying the material loading to maximize profit.

To optimally manage the energy consumption of a Hydrogen-Based steel plant under various price scenarios, sensitivity analysis is carried out to further increase profit under each price profile assumed. In the low price profile,when using a 100% efficiency fuel cell rated at 250 kW, and without restricting hydrogen intake, the profit of the steel plant only increases by €250,3 when compared to a 50 kW fuel cell with 50% efficiency. This is without considering operating costs of the fuel cell, which suggests that a fuel cell is not necessarily profitable to operate in a Hydrogen based steel plant.To overcome losses in the average price scenario, Hydrogen storage is essential. At least 700 kg of hydrogen should be available at the beginning of the production schedule to ensure positive profit. Flexibility is investigated for the peak price profile, which achieves the highest profit at € 271.072,65 for all the assumed scenarios. The plant reduces its consumption from 90 to 67.5 tonnes. Flexible operation displays profit margins up to €76,000 when assuming full capacity ($\epsilon = 1$) offered by the set of the flexible units. As ϵ increases, the plant reduces its total energy volume and shapes its consumption profile to maximize profit. The PEM offers the highest capacity, utilizing the peak price hour to sell its capacity.Under all price scenarios,the battery responds to electricity prices by charging at low prices and discharging at high prices to maximize profit for the industrial consumer. Fur-

thermore, demand response can be seen in various forms, such as changing the starting time of a batch cycle, increasing or decreasing the number of batch cycles, and varying the material loading for units depending on the price profiles.

The energy consumption data from Gurobi is used to model the units of the steel plant as time series loads to verify a radial network for the plant. These include the consumption of the units, and generation from fuel cell, battery, solar and wind.A radial network is proposed based on literature and discussion with DNV. Four 100 MVA transformers are proposed and contingency scenarios are generated until transformers supply the network. Thus, the main transformer ratings in the network are verified for the worst-case scenario (peak consumption) to ensure acceptable and safe operation within the steel plant. Results revealed that when two main transformers are taken out of service, the other two main transformers can reach 158.4% of their loading capacity in one timestep, which is acceptable for short-term durations. To analyze the impact of the steel plant on a transmission grid, the peak consumption value is modeled as a static load in a representative European high-voltage grid to carry out powerflow analysis. It reveals that the impact of the steel plant on the load capacity of the line and the voltage of the bus of the network depends on the location of the bus.

FUTURE WORKS

Future works for the thesis can be addressed in the following areas.In energy system modeling, using a smaller and more accurate resolution for the batch cycle duration of the units can provide a better representation of the production schedule and improve the quality of the objective function,which is possibly obtained when the model is applied to an existing steel plant. In power system modeling, representing the units using detailed steady state load models that include the converters can provide better insights on the plants behavior can a high voltage.For example, modeling the PEM electrolyzer similarly to the steady state load model of an electrolyzer with non-linear and operational constraints in [61].

BIBLIOGRAPHY

[1] United Nations Framework Convention on Climate Change (UNFCCC), *The paris agreement*, Accessed: 2025-02-10, 2015. [Online]. Available: https://unfccc.int/process-and-meetings/the-paris-agreement.

[2] International Energy Agency (IEA), *Global EV Outlook 2023*, Licence: CC BY 4.0, Accessed: 2025-02-10, Paris, 2023. [Online]. Available: https://www.iea.org/reports/global-ev-outlook-2023.

[3] M. Wei, C. McMillan, and S. Can, "Electrification of industry: Potential, challenges and outlook," *Current Sustainable/Renewable Energy Reports*, vol. 6, pp. 140–148, Dec. 2019. DOI: 10.1007/s40518-019-00136-1.

[4] International Renewable Energy Agency, *Decarbonising hard-to-abate sectors*, Accessed: September 20, 2024, 2024. [Online]. Available: https://horizoneuropencpportal.eu/sites/default/files/2024-06/irena-g7-decarbonising-hard-to-abate-sectors-2024.pdf.

[5] International Energy Agency, "Iron and steel technology roadmap," International Energy Agency, Paris, France, Energy Technology Perspectives, Oct. 2020, CC BY 4.0 Licence. [Online]. Available: https://www.iea.org/reports/iron-and-steel-technology-roadmap.

[6] World Economic Forum, "Steel – net-zero industry tracker 2024," World Economic Forum, Geneva, Switzerland, Net-Zero Industry Tracker, Dec. 2024, Includes sector–specific steel report, PDF download. [Online]. Available: https://reports.weforum.org/docs/WEF_Net_Zero_Industry_Tracker_2024_Steel.pdf.

[7] World Steel Association, "Hydrogen (h_2)-based ironmaking," World Steel Association, Brussels, Belgium, Fact Sheet, Feb. 2024, Part of World Steel fact-sheet series. [Online]. Available: https://worldsteel.org/wp-content/uploads/Fact-sheet-hydrogen-H2-based-ironmaking.pdf.

[8] J. Wang, Q. Wang, and W. Sun, "Optimal power system flexibility-based scheduling in iron and steel production: A case of steelmaking–refining–continuous casting process," *Journal of Cleaner Production*, vol. 414, p. 137 619, 2023, ISSN: 0959-6526. DOI: https://doi.org/10.1016/j.jclepro.2023.137619. [Online]. Available: https://www.sciencedirect.com/science/article/pii/S0959652623017778.

[9] L. Gan, T. Yang, X. Chen, G. Li, and K. Yu, "Purchased power dispatching potential evaluation of steel plant with joint multienergy system and production process optimization," *IEEE Transactions on Industry Applications*, vol. 58, no. 2, pp. 1581–1591, 2022. DOI: 10.1109/TIA.2022.3144652.

[10] X. Zhang, G. Hug, and I. Harjunkoski, "Cost-effective scheduling of steel plants with flexible eafs," *IEEE Transactions on Smart Grid*, vol. 8, no. 1, pp. 239–249, 2017. DOI: 10.1109/TSG.2016.2575000.

[11] G. Abeynayake, L. Cipcigan, and X. Ding, "Black start capability from large industrial consumers," *Energies*, vol. 15, no. 19, 2022, ISSN: 1996-1073. DOI: 10.3390/en15197262. [Online]. Available: https://www.mdpi.com/1996-1073/15/19/7262.

[12] A. Gholian, H. Mohsenian-Rad, and Y. Hua, "Optimal industrial load control in smart grid," *IEEE Transactions on Smart Grid*, vol. 7, no. 5, pp. 2305–2316, 2016. DOI: 10.1109/TSG.2015.2468577.

[13] A. Toktarova, L. Göransson, and F. Johnsson, "Design of Clean Steel Production with Hydrogen: Impact of Electricity System Composition," *Energies*, vol. 14, no. 24, pp. 1–21, Dec. 2021. [Online]. Available: https://ideas.repec.org/a/gam/jeners/v14y2021i24p8349-d700113.html.

[14] A. Bhaskar, R. Abhishek, M. Assadi, and H. N. Somehesaraei, "Decarbonizing primary steel production: Techno-economic assessment of a hydrogen-based green steel production plant in norway," *Journal of Cleaner Production*, vol. 350, p. 131 339, 2022, ISSN: 0959-6526. DOI: 10.1016/j.jclepro.2022.131339. [Online]. Available: https://www.sciencedirect.com/science/article/pii/S0959652622009659.

[15] V. Vogl, M. Åhman, and L. J. Nilsson, "Assessment of hydrogen direct reduction for fossil-free steelmaking," *Journal of Cleaner Production*, vol. 203, pp. 736–745, 2018, ISSN: 0959-6526. DOI: https://doi.org/10.1016/j.jclepro.2018.08.279. [Online]. Available: https://www.sciencedirect.com/science/article/pii/S0959652618326301.

[16] P. Su, Y. Zhou, H. Li, H. D. Perez, and J. Wu, "Cost-effective scheduling of a hydrogen-based iron and steel plant powered by a grid-assisted renewable energy system," *Applied Energy*, vol. 384, p. 125 412, 2025, ISSN: 0306-2619. DOI: 10.1016/j.apenergy.2025.125412. [Online]. Available: https://www.sciencedirect.com/science/article/pii/S0306261925001424.

[17] A. A. Mottahedi, S. Amani, and I. Metallurgy, "Using oxygen reaction as electricity saving in electric arc furnace steel making," 2009. [Online]. Available: https://api.semanticscholar.org/CorpusID:33413690.

[18] World Steel Association, *World Steel in Figures 2024*, Accessed: 2024-11-20, 2024. [Online]. Available: https://worldsteel.org/wp-content/uploads/World-Steel-in-Figures-2024.pdf.

[19] J. Schlegel, *The World of Steel*, en. Springer Fachmedien Wiesbaden, 2023. DOI: 10.1007/978-3-658-39733-3. [Online]. Available: https://doi.org/10.1007/978-3-658-39733-3.

[20] R. Wang, Y. Zhao, A. Babich, D. Senk, and X. Fan, "Hydrogen direct reduction (h-dr) in steel industry—an overview of challenges and opportunities," *Journal of Cleaner Production*, vol. 329, p. 129 797, 2021, ISSN: 0959-6526. DOI: 10.1016/j.jclepro.2021.129797. [Online]. Available: https://www.sciencedirect.com/science/article/pii/S095965262103972X.

[21] Y. Yang, L. Holappa, H. Saxen, and J. van der Stel, "Chapter 1.2 - ironmaking," in *Treatise on Process Metallurgy (Second Edition)*, S. Seetharaman, R. Guthrie, A. McLean, S. Seetharaman, and H. Y. Sohn, Eds., Second Edition, Elsevier, 2024, pp. 7–88, ISBN: 978-0-323-85373-6. DOI: https://doi.org/10.1016/B978-0-323-85373-6.00001-6. [Online]. Available: https://www.sciencedirect.com/science/article/pii/B9780323853736000016.

[22] A. Singh, R. Singh, and A. Singh, "Power quality issues of electric arc furnace and their mitigations -a review," *International Journal of Advanced Engineering Research and Science*, vol. 4, pp. 22–41, Jan. 2017. DOI: 10.22161/ijaers.4.4.4.

[23] H. Burghardt and G. Neuhof, *Stahlerzeugung*. Deutscher Verlag für Grundstoffindustrie, 1982. [Online]. Available: https://books.google.nl/books?id=TKSUwAEACAAJ.

[24] Midrex Technologies, Inc., "Direct from midrex: 1st quarter 2024," Midrex Technologies, Inc., Newsletter 1st Quarter 2024, 2024. [Online]. Available: https://www.midrex.com/wp-content/uploads/Midrex-DFM-1stQtr2024.final_.pdf (visited on 06/08/2025).

[25] J. Burgess. "Hybrit green hydrogen-for-steel project completes storage test," EUROMETAL. (Feb. 2025), [Online]. Available: https://eurometal.net/hybrit-green-hydrogen-for-steel-project-completes-storage-test/ (visited on 06/08/2025).

[26] K. Lee, S. Chang, and Y. Hong, "Continuous slab caster scheduling and interval graphs," *Production Planning Control*, vol. 15, pp. 495–501, Jul. 2004. DOI: 10.1080/09537280410001714279.

[27] SMS Group, *Skin-pass mill*, Accessed: 2024-11-25, 2024. [Online]. Available: https://www.sms-group.com/plants/skin-pass-mill.

[28] National Material Company, *What is steel pickling?* Accessed: 2024-11-25, 2018. [Online]. Available: https://www.nationalmaterial.com/what-is-steel-pickling/.

[29] TWI Ltd, *What is annealing? a complete process guide*, Accessed: 2024-11-25, 2024. [Online]. Available: https://www.twi-global.com/technical-knowledge/faqs/what-is-annealing.

[30] E. Morgan, *Hot rolled vs cold rolled steel: Overview and differences*, Accessed: 2025-01-21, Dec. 2021. [Online]. Available: https://www.rapiddirect.com/blog/hot-rolled-vs-cold-rolled-steel/.

[31] T. S. Nederland, *Hot rolled*, Accessed: 2025-01-21, 2025. [Online]. Available: https://products.tatasteelnederland.com/product-ranges/automotive/hot-rolled.

[32] T. S. Nederland, *Cold rolled*, Accessed: 2025-01-21, 2025. [Online]. Available: https://products.tatasteelnederland.com/product-ranges/automotive/cold-rolled.

[33] S. H. Sen, *6 common uses of cold rolled steel*, Accessed: 2025-01-21, Oct. 2024. [Online]. Available: https://www.steelhighsen.com/industry-news/6-common-uses-of-cold-rolled-steel.html#:~:text=Cold%20rolled%20steel%20is%20extensively%20used%20in%20the,as%20body%20panels%2C%20structural%20parts%2C%20and%20interior%20elements..

[34] S. Pfenninger and I. Staffell, "Long-term patterns of european pv output using 30 years of validated hourly reanalysis and satellite data," *Energy*, vol. 114, pp. 1251–1265, 2016. DOI: 10.1016/j.energy.2016.08.060. [Online]. Available: https://doi.org/10.1016/j.energy.2016.08.060.

[35] I. Staffell and S. Pfenninger, "Using bias-corrected reanalysis to simulate current and future wind power output," *Energy*, vol. 114, pp. 1224–1239, 2016. DOI: 10.1016/j.energy.2016.08.068. [Online]. Available: https://doi.org/10.1016/j.energy.2016.08.068.

[36] L. Thurner, A. Scheidler, F. Schafer, *et al.*, "Pandapower - an open source python tool for convenient modeling, analysis and optimization of electric power systems," *IEEE Transactions on Power Systems*, 2018, ISSN: 0885-8950. DOI: 10.1109/TPWRS.2018.2829021. [Online]. Available: https://arxiv.org/abs/1709.06743.

[37] R. Assunção, F. Eckl, C. P. Ramos, C. B. Correia, and R. C. Neto, "Oxygen liquefaction economical value in the development of the hydrogen economy," *International Journal of Hydrogen Energy*, vol. 62, pp. 109–118, 2024, ISSN: 0360-3199. DOI: 10.1016/j.ijhydene.2024.02.205. [Online]. Available: https://www.sciencedirect.com/science/article/pii/S036031992400627X.

[38] U.S. Department of Energy. "Can water usage for electrolysis pose problems in parts of the united states currently facing water shortages?" Accessed: 2025-04-05, Office of Energy Efficiency & Renewable Energy. (n.d.), [Online]. Available: https://www.energy.gov/eere/fuelcells/can-water-usage-electrolysis-pose-problems-parts-united-states-currently-facing.

[39] J. Bolotova. "Steel hrc prices inch upward across europe," EUROMETAL. (Feb. 2025), [Online]. Available: https://eurometal.net/steel-hrc-prices-inch-upward-across-europe/ (visited on 06/08/2025).

[40] D. Kahramanova. "European crc, hdg prices increase on limited availability," EUROMETAL. (Mar. 2025), [Online]. Available: https://eurometal.net/european-crc-hdg-prices-increase-on-limited-availability/ (visited on 06/08/2025).

[41] J. D. Jong. "Annual market update 2023: Electricity market review focused on the netherlands and germany." Accessed: 2025-04-05, TenneT. (Jan. 2025), [Online]. Available: https://www.tennet.eu/nl-en/news/annual-market-update-2023-electricity-market-review-focused-netherlands-and-germany-including.

[42] ENTSO-E. "Entso-e transparency platform – day-ahead market prices (netherlands bzn)." Accessed: 2025-06-03. (2023), [Online]. Available: https://newtransparency.entsoe.eu/market/energyPrices?appState=%7B%22sa%22%3A%5B%22BZN%7C10YNL----------L%22%5D%2C%22st%22%3A%22BZN%22%2C%22mm%22%3Atrue%2C%22ma%22%3Afalse%2C%22sp%22%3A%22HALF%22%2C%22dt%22%3A%22TABLE%22%2C%22df%22%3A%222023-01-01%22%2C%22tz%22%3A%22CET%22%7D (visited on 06/03/2025).

[43] A. Burke, J. Ogden, L. Fulton, and S. Cerniauskas, "Hydrogen storage and transport: Technologies and costs," UC Davis: Hydrogen Pathways Program, Tech. Rep., 2024, Retrieved from eScholarship, accessed 2025-04-04. [Online]. Available: https://escholarship.org/uc/item/83p5k54m.

[44] Y. Astriani, W. Tushar, and M. Nadarajah, "Optimal planning of renewable energy park for green hydrogen production using detailed cost and efficiency curves of pem electrolyzer," *International Journal of Hydrogen Energy*, vol. 79, pp. 1331–1346, 2024, ISSN: 0360-3199. DOI: https://doi.org/10.1016/j.ijhydene.2024.07.107. [Online]. Available: https://www.sciencedirect.com/science/article/pii/S0360319924027782.

[45] P. C. Sen, *Principles of Electric Machines and Power Electronics*, 2nd ed. New York: John Wiley & Sons, 1996, ISBN: 0471022950.

[46] *Abb drives in metals: Medium voltage drives for improved product quality and process control*, Revision A, ABB Group, Zurich, Switzerland, 2008. [Online]. Available: https://library.e.abb.com/public/fa03734fae60f940c1257b0c00551e7c/ABB%20drives%20in%20metals_RevA_2008.pdf.

[47] ABB, "Hot annealing and pickling line with 2-stand inline mill," ABB (China) Limited, Business Unit Metals, Beijing, P. R. China, Installed Base Reference CN2009062603, Jun. 2009, Accessed 21 May 2025. [Online]. Available: https://search.abb.com/library/Download.aspx?DocumentID=CN2009062603&LanguageCode=en&Action=Launch (visited on 05/21/2025).

[48] N. Zecca, P. D. Cobden, L. Lücking, and G. Manzolini, "Sewgs integration in a direct reduction steelmaking process for co_2 mitigation," *International Journal of Greenhouse Gas Control*, vol. 130, p. 103 991, 2023, ISSN: 1750-5836. DOI: 10.1016/j.ijggc.2023.103991. [Online]. Available: https://www.sciencedirect.com/science/article/pii/S1750583623001615.

[49] T. Astoria and M. Hargreaves. "Electrical heating of midrex® process gases." Tech Article, Midrex Technologies, Inc. (Sep. 2023), [Online]. Available: https://www.midrex.com/tech-article/electrical-heating-of-midrex-process-gases/ (visited on 05/19/2025).

[50] C. Zhao, Q. Jiang, and D. Liu, "Flexible power supply system of ac electric arc furnace," *Journal of Modern Power Systems and Clean Energy*, vol. 11, no. 2, pp. 622–633, 2023. DOI: 10.35833/MPCE.2021.000414.

[51] A. Hassan, A. ABOU-GHAZALA, and A. MEGAHED, "Field-verified integrated eaf-svc-electrode positioning model simulation and a novel hybrid series compensation control for eaf," *TURKISH JOURNAL OF ELECTRICAL ENGINEERING COMPUTER SCIENCES*, vol. 26, pp. 363–377, Jan. 2018. DOI: 10.3906/elk-1702-215.

[52] ABB Switzerland Ltd., "Acs 6000 medium voltage ac drives for control of 3–27 mw motors up to 3.3 kv," ABB Switzerland Ltd., Medium Voltage Drives, Turgi, Switzerland, Product brochure 3BHT 490 399 R0001 Rev. D, 2008, Revision D. [Online]. Available: https://library.e.abb.com/public/d30de1862c34d04dc1257b0c00551f88/ACS_6000_EN_RevD-3.pdf (visited on 05/19/2025).

[53] ABB Switzerland Ltd., "Acs1000 medium voltage drive catalog: The flexibility you require. the reliability you expect," ABB, Zurich, Switzerland, Product brochure 3BHT490400R0001, 2014, Accessed 25 May 2025. [Online]. Available: https://search.abb.com/library/Download.aspx?DocumentID=3BHT490400R0001&LanguageCode=en.

[54] Cummins Inc., "Hylyzer® 500 electrolyzer system – specification sheet," Cummins Inc., Columbus, Indiana, USA, Product specification, Aug. 2021, Accessed 25 May 2025. [Online]. Available: https://www.cummins.com/sites/default/files/2021-08/cummins-hylyzer-500-specsheet.pdf.

[55] ABB Switzerland Ltd., "Mcr1000 medium current rectifier: 5 ka to 200 ka up to 1,000 vdc," ABB Switzerland Ltd., High Power Rectifiers, Switzerland, Factsheet 3BHS546772E01 Rev. A, Sep. 2021, Accessed 25 May 2025. [Online]. Available: https://search.abb.com/library/Download.aspx?DocumentID=3BHS546772E01&LanguageCode=en&DocumentPartId=&Action=Launch.

[56] C. S. Chen, Y. D. Lee, C. T. Hsu, D. S. Ting, and C. C. Shen, "Power quality assessment of a hot strip mill with cycloconverter drive systems," in *2007 IEEE Industry Applications Annual Meeting*, 2007, pp. 9–16. DOI: 10.1109/07IAS.2007.22.

[57] GE Digital Energy (GE Vernova), *Transformers: Three phase up to 1500mva with primaryplus™*, Brochure, GEA-12718C(E), accessed 18 July 2025, GE VernovaInc., Atlanta, GA, USA, 2014. [Online]. Available: https://www.gevernova.com/grid-solutions/sites/default/files/resources/products/brochures/primaryequip/transformers.pdf.

[58] "Ieee guide for loading mineral-oil-immersed transformers and step-voltage regulators," *IEEE Std C57.91-2011 (Revision of IEEE Std C57.91-1995)*, pp. 1–123, 2012. DOI: 10.1109/IEEESTD.2012.6166928.

[59] S. Fliscounakis, P. Panciatici, F. Capitanescu, and L. Wehenkel, "Contingency ranking with respect to overloads in very large power systems taking into account uncertainty, preventive, and corrective actions," *IEEE Transactions on Power Systems*, vol. 28, pp. 4909–4017, Nov. 2013. DOI: 10.1109/TPWRS.2013.2251015.

[60] C. Josz, S. Fliscounakis, J. Maeght, and P. Panciatici, *Ac power flow data in matpower and qcqp format: Itesla, rte snapshots, and pegase*, 2016. arXiv: 1603.01533 [math.OC]. [Online]. Available: https://arxiv.org/abs/1603.01533.

[61] A. De Corato, M. Ghazavi, S. Riaz, and P. Mancarella, "Hydrogen electrolyzer load modelling for steady-state power system studies," *IEEE Transactions on Power Delivery*, vol. PP, pp. 1–11, Sep. 2023. DOI: 10.1109/TPWRD.2023.3315749.

A

APPENDIX

A.1. A1:GITHUB

This GitHub repository contains the codes used to run the simulations, a summary of the main results for each scenario, the calculations for the H2.

A.2. A2:SHAREPOINT

Inside the sharepoint link are all of the results of the optimization of all 40 scenarios,that include energy consumption, material storage, optimal schedule, decision variable in excel, pkl files for pandapower,battery capacity, fuel cell, and oxygen supply to EAF. the folders that represent each scenario.

A.3. A2:SUMMARY OF RESULTS

Table A.1 highlights the main results of the 40 scenarios generated for the energy system modeling. Carbon emissions depend on the final amount of steel produced which for a total steel production of 860 tonnes amount to 0.0236 tCO_2.Highest profit is achieved at €271,072.65 for the Peak Price Scenario with a flexibility of ε=1.0. All simulations converged with an MIGAP of 0.1%.

A

Table A.1: Scenarios Generated and Main Results Summarized

Operation Mode	CR [t]	HB [t]	Profit	CO_2 Emissions [t]	Solve Time [s]
Fixed Price	722	100	€204,136.70	0.0235	444.09
Fixed Price (Renewables 1 MW)	722	100	€208,175.70	0.0235	466.64
Fixed Price (Renewables + Battery 1 MW)	722	100	€208,889.80	0.0235	337.54
Fixed Price (Renewables + Fuel Cell 1 MW)	722	100	€210,364.40	0.0235	503.13
Fixed Price (Renewables + Battery + Fuel Cell 1 MW)	722	100	€211,078.43	0.0235	430.82
Low Prices	722	100	€262,185.20	0.0235	367.90
Low Prices (Fuel Cell = 100 kWh)	722	100	€262,364.60	0.0235	354.86
Low Prices (Fuel Cell = 150 kWh)	722	100	€262,409.85	0.0235	394.60
Low Prices (Fuel Cell = 200 kWh)	722	100	€262,409.85	0.0235	1863.35
Low Prices (Fuel Cell eff = 0.7, Fuel Cell = 200 kWh)	722	100	€262,416.27	0.0235	386.00
Low Prices (Fuel Cell eff = 0.8, Fuel Cell = 200 kWh)	722	100	€262,422.70	0.0235	543.71
Low Prices (Fuel Cell eff = 0.9, Fuel Cell = 200 kWh)	722	100	€262,426.90	0.0235	557.64
Low Prices (Fuel Cell eff = 0.9, Fuel Cell = 250 kWh)	722	100	€262,429.10	0.0235	611.58
Low Prices (Fuel Cell eff = 1.0, Fuel Cell = 250 kWh)	722	100	€262,435.50	0.0235	197.63
Average Prices	722	100	-€97,795.70	0.0235	519.46
Average Prices (H_2=0.1)	741	100	-€75,069.23	0.0235	413.04
Average Prices (H_2=0.2)	741	100	-€64,786.20	0.0235	519.07
Average Prices (H_2=0.3)	741	100	-€54,503.14	0.0235	374.37
Average Prices (H_2=0.4)	741	100	-€41,142.00	0.0235	544.23
Average Prices (H_2=0.5)	741	100	-€30,921.87	0.0235	503.52
Average Prices (H_2=0.6)	741	100	-€20,701.70	0.0235	582.65
Average Prices (H_2=0.7)	760	100	-€154.30	0.0236	765.03
Average Prices (H_2=0.8)	760	100	€10,021.70	0.0236	959.23
Average Prices (H_2=0.9)	760	100	€20,197.57	0.0236	1089.70
Average Prices (H_2=1.0)	760	100	€37,870.50	0.0236	1784.30
Peak Prices	722	100	€166,602.10	0.0235	461.09
Peak Prices (Unbounded)	722	90.79	€194,171.20	0.0215	441.82
Peak Prices-Flexibility (ε=0.1)	722	85.46	€231,859.70	0.0215	632.75
Peak Prices-Flexibility (ε=0.2)	722	80.12	€244,134.95	0.0215	500.18
Peak Prices-Flexibility (ε=0.3)	722	72.33	€252,203.70	0.0215	473.71
Peak Prices-Flexibility (ε=0.4)	722	67.95	€259,208.10	0.0215	466.98
Peak Prices-Flexibility (ε=0.5)	722	67.95	€265,142.66	0.0215	520.50
Peak Prices-Flexibility (ε=0.6)	722	67.95	€266,489.72	0.0215	525.46
Peak Prices-Flexibility (ε=0.7)	722	67.95	€267,714.87	0.0215	423.79
Peak Prices-Flexibility (ε=0.8)	722	67.95	€268,874.40	0.0215	498.96
Peak Prices-Flexibility (ε=0.9)	722	67.95	€270,047.30	0.0215	507.32
Peak Prices-Flexibility (ε=1.0)	722	67.95	€271,072.65	0.0215	524.75